Adriano José Simões Brás

Licenciatura em Engenharia de Materiais

Production of UCST-like thermosensitive membranes by colloidal electrospinning

Dissertação para obtenção do Grau de Mestre em
Engenharia de Materiais

Orientador: Doutora Paula Isabel Pereira Soares,
Investigadora em Pós-doutoramento,
CENIMAT-I3N Departamento de Ciência dos Materiais,
Faculdade de Ciências e Tecnologia da Universidade Nova de Lisboa
Co-orientador: Doutora Coro Echeverria Zabala,
Investigadora em Pós-doutoramento,
CENIMAT-I3N Departamento de Ciência dos Materiais,
Faculdade de Ciências e Tecnologia da Universidade Nova de Lisboa

Júri:

Presidente: Professor Doutor João Pedro Botelho Veiga

Arguente: Professora Doutora Ana Cataria Bernardino Baptista

Vogal: Professora Doutora Paula Isabel Pereira Soares

Setembro 2017

FACULDADE DE CIÊNCIAS E TECNOLOGIA
UNIVERSIDADE NOVA DE LISBOA

Production of UCST-like thermosensitive membranes by colloidal electrospinning

Acknowledgments/Agradecimentos

No início fui bastante resistente em fazer esta página de agradecimentos, pois tenho receio de ser injusto ao me esquecer de alguém que também foi muito importante ao longo destes cinco anos do curso. O meu crescimento / aprendizagem só foi possivel pelas muitas trocas de experiências reflexivas e partilhadas. A todos eles o meu enorme agradecimento – “Muito Obrigada”.

Começo por agradecer à minha orientadora, Doutora Paula Soares, pela disponibilidade, pela paciência que teve com as minhas inseguranças, pelo tempo despendido, pelas sugestões, apoio e conhecimentos transmitidos.

Agradeço à minha co-orientadora, Coro Echeverria Zabala, por toda a ajuda da parte experimental, pela disponibilidade e paciência, pelo conhecimento que me transmitiu, pelas críticas construtivas que me levavam sempre a querer fazer melhor e também pelas muitas correções na parte escrita.

Um enorme agradecimento ao Doutor João Paulo Borges, coordenador de curso, pela sua capacidade de comunicação, de empatia e segurança transmitida.

À doutora Suzete Fernandes, agradeço todas as indicações dadas em laboratório, pela paciência, simpatia e apoio prestado.

Ao Professor João Canejo e à Ana Almeida o meu agradecimento pelas conversas simpáticas e pelo apoio no laboratório.

À Maria Augusta e a todas as pessoas do laboratório, um obrigado pela empatia pelo apoio e por tornarem o ambiente de trabalho agradável.

Ao meu colega Jaime Faria, obrigado pelos apontamentos e pela amizade demonstrada. Obrigado por toda a ajuda prestada, desde artigos recomendados a dicas sobre como fazer as experiências de electrospinning de uma maneira fácil, rápida e eficaz.

Aos meus colegas do laboratório, Ricardo Matos, Renato Martins, Paula Martins, Miguel Baptista e à Catarina Chaparro, o meu agradecimento pelos bons momentos que passamos juntos e pelo apoio e motivação que me deram nesta última parte do curso.

Aos meus colegas e amigos durante todos estes cinco anos, Volodymyr Ulyanovskyy e Diogo Gomes, o meu obrigada pelas conversas, pela amizade demonstrada, pelos momentos de lazer, mas também os de estudo em que a troca de conhecimentos e partilha se tornaram indispensáveis para o nosso sucesso. Espero que esta amizade continue para a vida.

Por último, mas mais importante, quero expressar o meu enorme agradecimento a toda a minha família, pais irmão, avós, tias e primos que sempre me apoiaram e aturaram em todos os bons e maus momentos. Obrigado por toda a compreensão que tiveram.

Abstract

In the last decades, the focus in materials science has been the development of multifunctional materials with enhanced properties as “smart materials”. This new generation of materials possess adaptive capabilities to external stimuli, that is, they can change their properties due to an external stimulus. For instance, over the last years there has been an increasing interest in thermosensitive microgels, because of their potential applications on many distinct fields, mainly in biomedical engineering.

This dissertation reports on the development of polymeric composite membranes toward smart systems. The production of the composite membranes was achieved by the confinement of positive thermosensitive microgels that might act as active sites inside a polymeric fiber, by means of colloidal electrospinning process, which is a variant of the classical electrospinning methodology.

For the production of this composite membranes, first poly(acrylamide) and poly(acrylamide-acrylic acid) microgels were synthesized using inverse emulsion polymerization technique. The obtained UCST microgels were characterized in terms of their morphology, swelling properties and chemical structure. Then, the obtained microgels were dispersed in the polymeric fiber template solution (Polyvinylpyrrolidone /Ethanol) and further electrospun by means of colloidal electrospinning.

Previous works already report the encapsulation of PNIPAAm microgels in electrospun fibers, and there is also reports of the synthesis of positive thermosensitive poly(acrylamide-acrylic acid) microgels. The novelty of this dissertation is the encapsulation of these positive microgels inside electrospun fibers.

Tensile test experiments infer that the addiction of microgels improves the mechanical properties of composite membranes.

The confinement of the microgels were further confirmed by SEM, resulting on a “*bead-on-string*” fiber morphology. The presence of water in the solvent system of the polymeric solution revealed to be a crucial factor in the confinement of the microgels inside the fibers, since it not only stabilized the microgels dispersed in the polymeric solution, but also reduced significantly the fiber diameters. Since the size of these “beads” on the fiber is tunable, this could mean that this system could have the ability to tune the roughness of the fibers, hydrophobicity and wettability.

This results in a very versatile system with potential development for various applications.

Keywords: PVP; PAAm; PAAc; Microgels; Colloidal Electrospinning; Fibers.

Resumo

Nas últimas décadas, um dos focos da ciência dos materiais tem sido o desenvolvimento de “materiais inteligentes”, multifuncionais e com propriedades melhoradas. Esta nova geração de materiais possui capacidades adaptativas a estímulos externos. Por exemplo, nos últimos anos tem havido um interesse crescente em microgeís termossensíveis pelas suas varias potenciais aplicações em diversos campos, com principal foco na engenharia biomédica.

Esta dissertação relata sobre o desenvolvimento de membranas compósitas poliméricas para sistemas inteligentes. A produção destas membranas foi conseguida pelo confinamento de microgeís termossensíveis dentro de uma fibra polimérica, através de um processo de eletrofiação coloidal.

Para a produção destas membranas compósitas, foram sintetizados microgeís de poliacrilamida e ácido poliacrílico usando a técnica de polimerização em emulsão inversa. Os microgeís obtidos foram caracterizados em termos de sua morfologia, termossensibilidade e estrutura química. Estes microgeís foram dispersos numa solução polimérica (Polivinilpirrolidona/Etanol) e posteriormente submetidos eletrofiação coloidal.

Trabalhos anteriores já relatam sobre o encapsulamento de microgeís de PNIPAAm em fibras electrofiadas, e também sobre a síntese de microgeís de poli(acrilamida-ácido acrílico) com termossensibilidade positiva. A novidade desta dissertação é o encapsulamento destes microgéis de poli(acrilamida-ácido acrílico) em fibras electrofiadas.

Os ensaios mecânicos revelaram que a adição de microgeís melhora as propriedades mecânicas das membranas compósitas.

O confinamento dos microgeís foi confirmado por SEM (*scanning electron microscope*), resultando em uma morfologia de fibra *"bead-on-string".* A presença de água como solvente da solução polimérica revelou ser importante no confinamento dos microgeís, uma vez que não só os estabilizou na solução polimérica, mas também reduziu significativamente os diâmetros das fibras obtidas. Visto que o tamanho dos microgeís que foram confinados na fibra é ajustável, isto significa que este sistema pode ter a capacidade de modificar a rugosidade das fibras, a hidrofobia e a molhabilidade.

Resultando assim num sistema muito versátil e com potencial de desenvolvimento para variadas aplicações.

Palavras chave: PVP; PAAm; PAAc; Microgéis; Electrofiação coloidal; fibras.

Contents

Acknowledgments/Agradecimentos v
Abstract vii
Resumo ix
Contents xi
List of Figures xiii
List of Tables xv
Abbreviations xvii
Symbols xix
1 Introduction 1
1.1 Brief introduction: Smart functional materials 1
1.2 Microgel as a smart colloidal polymeric system 1
1.2.1 Microgels 1
1.2.2 Thermosensitive microgels 2
1.3 Functional composite membranes as smart multifunctional systems: Colloidal electrospinning 4
2 Materials and methods 7
2.1 Materials 7
2.2 Synthesis of Poly(acrylamide) microgels 7
2.3 Colloidal-Electrospinning 7
2.4 UV cross-linking method 8
2.5 Characterization techniques 8
3 Results and Discussion 9
3.1 PAAm-AAc microgels as active sites 9
3.1.1 Morphology 9
3.1.2 Structural characterization 11
3.1.3 Thermogravimetric Analysis 13
3.1.4 Swelling properties and thermoresponsiveness 14
3.2 Production of composite membranes 15
3.2.1 Confinement microgels of microgels (active sites) into PVP fibers 16
3.2.2 Analysis of the mechanical properties. Influence of the microgels 22

4 Conclusions and Future Perspectives 25
5 References 27
6 Supporting Information 31
6.1 Vacuum distillation 31
6.2 Synthesis of Poly(acrylamide) microgels 32
6.3 Polymerization reaction 33
6.4 Determination of swelling properties using Dynamic Light Scattering 35
6.5 Determination of swelling properties using Optical Microscope 36
6.6 Membrane pre-selection with Optical Microscope 37

List of Figures

Figure 1.1-Representation of a chemical and a physical gel. 2
Figure 1.2-Illustration of typical positive thermoresponsive behavior. 3
Figure 1.3-Chemical structure of: a) Acrylamide; b) Acrylic Acid 3
Figure 1.4-P(AAm -AAc) matrix at low and high temperatures. 3
Figure 1.5-Schematic illustration of a colloidal electrospinning setup. The green circles represent the colloid phase. 5
Figure 3.1-SEM micrographs of PAA microgels with 0 wt.% AAc (A), PAA-AAc with 5 wt.% AAc (B), PAA-AAc with 10 wt.% AAc (C) and PAA-AAc with 15 wt.% AAc (D). 10
Figure 3.2-Size distribution of the poly(acrylamide-acrylic acid) microgels 10
Figure 3.3-Influence of the AAc concentration on the size of the poly(Acrylamide-Acrylic acid) microgels. 11
Figure 3.4- FT-IR spectra of the poly(AAm) and poly(AAm-AAc) microgel samples with 5wt.% AAc, 10wt.% AAc and 15wt.% AAc. 12
Figure 3.5-Thermal degradation for the microgel samples of PAAm (black) and co-polymer P(AAm-AAc)-5 wt.% (red), P(AAm-AAc)-10 wt.% (yellow), P(AAm-AAc)-15 wt.% (green). 13
Figure 3.6-Representative SEM micrographs of composite membranes obtained for the polymeric solution of 14 wt.% PVP in ethanol with 20 % (w/w) microgels(A) and 10 wt.% PVP in ethanol with 10% (w/w) microgels (B). 19
Figure 3.7- Representative SEM micrographs of composite membranes obtained for the polymeric solution of 14 wt.% PVP in ethanol and water with 10 wt.% (C) and 20 wt.% microgels (D) and 10 wt.% PVP with 10 wt.% (E) and 20 wt.% microgels (F) 21
Figure 3.8-(A) Representative Stress/strain curves for 10 wt.% PVP composite membranes containing 0, 10 and 20% microgels (MG) without water in their composition. (B) Table with Mechanical properties obtained from the mechanical tests 22
Figure 3.9-(A) Representative Stress/strain curves for 10 wt.% PVP composite membranes containing 0, 10 and 20% microgels (MG) with water in their composition. (B) Table with Mechanical properties obtained from the mechanical tests 23
Figure 6.1- Vacuum distillation set-up; 1-heater; 2- round bottom flask; 3- thermometer; 4- condenser; 5-round bottom flask; 6- Vacuum inlet;- adapted from [56] 31
Figure 6.2-Microgel synthesis set-up. 32
Figure 6.3-Microgels in inverse emulsion (w/o) 32
Figure 6.4-Polymerization reaction scheme. 1) and 2) Thermal activation of the initiator/Initiation; 3) Propagation; 4) Termination 33
Figure 6.5-Termination that leads to chain branching 34
Figure 6.6- Evolution of the hydrodynamic diameter (Dh) with temperature for simple Polyacrylamide microgels (0% AAc) and PAA-AAc 5% AAc, 10% AAc 35
Figure 6.7-Samples seen through the Optic Microscope with increasing temperature. 36
Figure 6.8-Influence of the temperature on the swelling of the microgels with 5 wt.% AAc 37

Figure 6.9-Microscopic image of fused fibers for the polymeric solution with 10 wt.% PVP in ethanol with 20 % w/w MG 37
Figure 6.10-Microscopic image of fused fibers for the polymeric solution with 14 wt.% PVP in ethanol with 10 % w/w MG 38

List of Tables

Table 2.1-Compositions of the synthesized PAA-AAc copolymer microgels 7
Table 3.1-All the different solution parameters.* The microgels used in the production of this set of composite membranes were poly(acrylamide) (0% acrylic acid). (See SEM image in Figure 3.1A) 17
Table 3.2-Results for the fiber mats of 14 wt.% PVP in ethanol with 20 % (w/w) of microgels and 10 wt.% PVP in ethanol with 10 % (w/w) of microgels (without water). 18
Table 3.3- Results for the fiber mats of 14 wt.% PVP in ethanol and water with 10% (w/w) of microgels and with 20% (w/w) of microgels. 20

Abbreviations

AAc	Acrylic Acid
AMPA-d	2,2'-Azobis(2-methylpropionamidine) dihydrochloride
DLS	Dynamic Light Scattering
EtOH	Ethanol
FIB	Focused Ion Beam
FTIR	Fourier transform infrared
LCST	Lower Critical Solution Temperature
MBA	N,N-methylene bis-acrylamide
MFD	Mean fibre diameter
MG	Microgel
P(AAm-AAc)	Poly(acrylamide-acrylic acid)
PEO	Poly(ethylene oxide)
PNIPAAm	Poly(*N*-isopropylacrylamide)
PVP	Polyvinylpyrrolidone
RH	Relative Humidity
SEM	Scanning Electron Microscopy
TCD	Tip-to-collector distance
TGA	Thermogravimetric analysis
UCST	Upper Critical Solution Temperature
UTS	Ultimate Tensile Strength
UV	Ultraviolet
VPTT	Volume Phase Transition Temperature

Symbols

D_h	Hydrodynamic Diameter
M_w	Molecular weight
ε	Extension
E	Young's Modulus
σ	Stress

1 Introduction

1.1 Brief introduction: Smart functional materials

In the last decades, the focus in materials science has been the development of multifunctional materials with enhanced properties as smart materials. This new generation of materials possess adaptive capabilities to external stimuli. However, this definition is too general, as almost all materials respond or react in some way to external stimuli, so clearly there is a fine line dividing “smart” and conventional materials. The difference is in its response to the stimuli, this “smart behavior” occurs when a material is exposed to an external stimulus and reacts in a useful and reliable way.

These capabilities can provide numerous possible applications for these materials and structures in many distinct fields such as aerospace, manufacturing, civil infrastructure systems, biomedical, etc.

Over the last years, research on these smart materials has been directed toward the production of systems that can release drugs [1, 2], present self-memory properties (actuators) [3], have the ability to self-heal [4, 5] or even smart sensing materials [6].

Recent works in the Soft and Biofunctional Materials (SBM) research groups already explored the synthesis and confinement of microgels inside electrospun fibers. Marques *et al.* reports about the synthesis of PNIPAAm/Chitosan stimuli-responsive microgels and their confinement inside poly(ethylene oxide (PEO)/Water/Ethanol (EtOH) electrospun fibers. [7] A statistical analysis of the electrospinning parameters was done by applying a design of experiments (DoE) in order to minimize the fiber diameters and get the microgels encapsulated. The PNIPAAm/Chitosan microgels were successfully confined inside 63±25 nm electrospun fibers, presenting a ‘bead-on-string’ morphology.

Faria *et al.* reported about the synthesis of PNIPAAm/Acrylic acid microgels and their confinement inside electrospun fibers of poly(N-vinylpyrrolidone) (PVP). These microgels already presented a VPTT (volume phase transition temperature) more suitable for physiological applications. For the PVP membranes, an UV irradiation treatment was applied to prevent dissolution. It was also focused the study of the membranes and their swelling. [8]

In this work we take advantage of these recent developments in the production of smart membranes to increase their functionality by incorporating actives sites to these membranes.

Those active sites will be polymeric microgel particles that are able to change their volume when stimulated with temperature.

1.2 Microgel as a smart colloidal polymeric system

1.2.1 Microgels

Microgels are intramolecularly cross-linked polymer particles in colloidal size range that have the ability to swell and shrink in suitable solvents. This soft material was first described by Baker in 1949 [9]. In the last 15 years microgels have been much studied due to their small size, which makes them very effective and fast to respond to external stimuli, compared to macroscopic gels [10]. Depending on the composition, microgels can exhibit volume transition and swell or shrink in response to external stimuli such as temperature, pH and light, among others [11-13]. Thus, polymeric microgels are receiving

increasing attention due to their potential applications in numerous fields, such as drug delivery, sensors, catalysis, chemical separation and enzyme immobilization [14-17].

Generally, microgels can be classified as chemical or physical, depending on the nature of their cross-links (Figure 1.1). In the case of chemical microgels, their tridimensional network is achieved by permanent covalent bonding between polymeric chains, resulting in a polymeric network that is insoluble in any solvent, being only able to swell in suitable solvents [14].

Physical microgels are formed by the growth of physical connected aggregates. Depending on the nature of each system, the junctions may be crystalline regions, hydrogen bonds, ionic and van der Waals forces. These physical microgels, unlike the chemical ones, can be dissolved [14] and present reversibility upon heating/cooling.

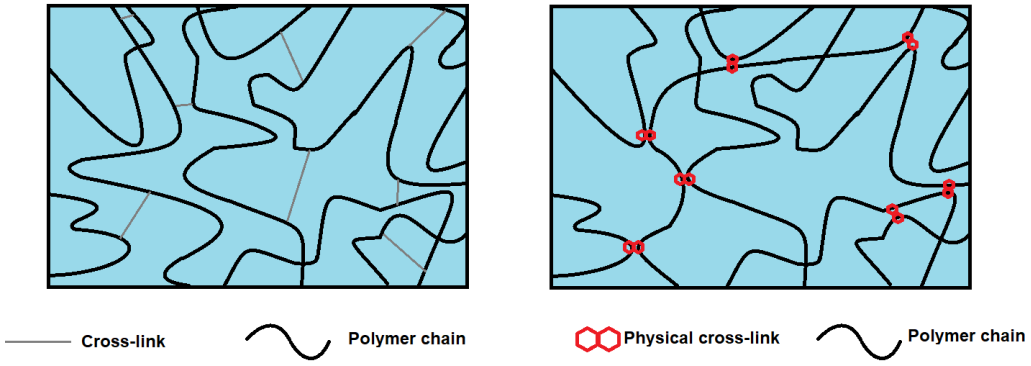

Figure 1.1-Representation of a chemical and a physical gel.

As mentioned before, microgels present several advantages relatively to hydrogels (or macrogels): i) faster to respond to stimuli; ii) good colloidal stability; iii) higher surface area to volume ratio; iv) good tunability; v) smaller size allows a less invasive administration [18].

1.2.2 Thermosensitive microgels

There are two types of thermally responsive microgels, those which exhibit a lower critical solution temperature (LCST) like poly(N-isopropylacrylamide) or poly(vinylcaprolactone) microgels that collapse by heating (negative thermosensitivity), and those which exhibit an upper critical solution temperature (UCST) and swell with the increasing temperature (positive thermosensitivity, Figure 1.2). The temperature responsible for the volume change is called Volume Phase Transition Temperature (VPTT) that is closely related to the LCST/UCST [19, 20].

Microgels based on PNIPAAm (poly(N-Isopropylacrylamide)) have been extensively studied due to their ability to swell at low temperature and collapse when the temperature increases. In this system, the volume phase transition (VPT) is driven by hydrophobic interactions between macromolecules. As mention before, these kind of systems are suitable for drug delivery applications among others [21]. However, for this application an opposite behavior would be more suitable, that is, the microgel should remain collapsed at room temperature to trap the drug inside, and when increasing the temperature, the microgel should swell and thus release the drug [22]. This type of thermoresponsive microgels are known as positive thermoresponsive.

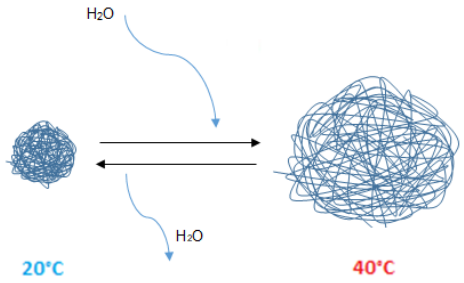

Figure 1.2-Illustration of typical positive thermoresponsive behavior.

Despite UCST-like microgels have been less studied, this positive thermoresponsive behavior can be found in chemically crosslinked poly(acrylamide-acrylic acid) copolymer microgels (Poly(AAm-AAc)). The synthesis of thermoresponsive microgels with this polymer system was already reported by Echeverria *et al.* and Ruiz *et al.* that will be also used for the present dissertation [22, 23].

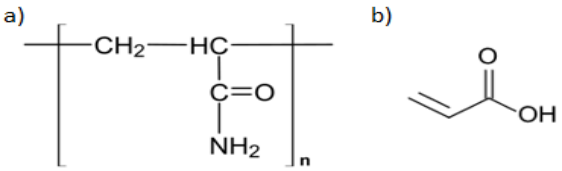

Figure 1.3-Chemical structure of: a) Acrylamide; b) Acrylic Acid

This UCST microgels constituted by chains of both poly(acrylamide) (PAAm) and poly(acrylic acid) (PAAc) (Figure 1.3) show a swelling behavior when heated that is not comparable with the swelling observed in neat poly(acrylamide), which is not temperature responsive, or with neat poly(acrylic acid) microgels [23].

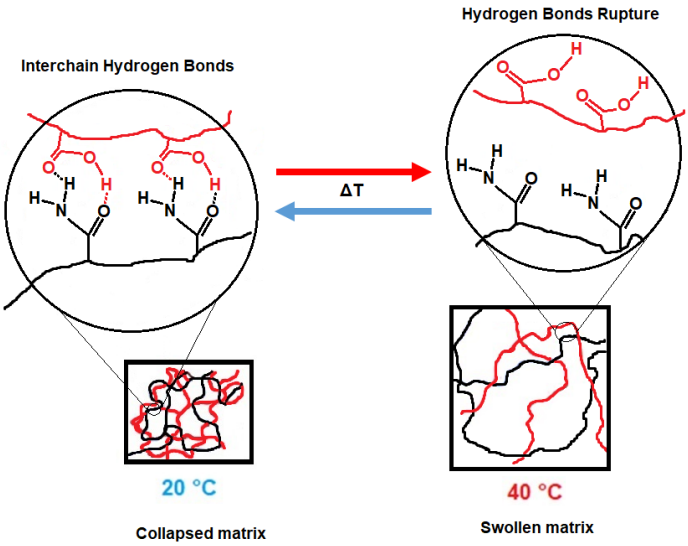

Figure 1.4-P(AAm -AAc) matrix at low and high temperatures.

Figure 1.4 depicts the PAAm/PAAc matrix configuration of the microgel polymeric network at high and low temperatures. As it has been reported by Peppas *et al.* [24] and Bouillot and Vincent [25], their volume change with temperature is driven by hydrogen bonding causing the microgel to shrink at temperatures below the UCST and swell at temperatures above [22]. These hydrogen bonds are strongly bound at low temperatures, but because it is just a secondary bond, as the temperature increases, these bonds weaken and rupture giving rise to a hydrophilic front and resulting in the miscibility of the system. This phenomenon is called “zipper effect” [26] and results in the reduction of the elastic tension that stabilizes the microgel, favoring the polymer swelling [23, 27]. However, unlike PNIPAM where the volume phase transition spans a range of only 2-3 degrees, the transition in PAA elapses at an interval of about 30°C [27].

1.3 Functional composite membranes as smart multifunctional systems: Colloidal electrospinning

Polymeric membranes are used for multiple biomedical applications and lead the membrane separation industry market. For instance, they can be used to provide sophisticated filtration devices for the medical industry. The production of polymeric fiber membranes can be achieved by several different methods (like chemical vapor deposition, wet spinning, dry spinning, melt spinning, etc), but when considering the production method of these stimuli-responsive multifunctional systems, electrospinning technique comes as an advantage since not only it allows the incorporation of active sites (like microgels) [28] but also enhances the sensitivity of the entire system to external stimuli due to the ease of material combination, extremely large surface area and porosity of the fibers [29, 30].

Electrospinning is a simple and cost-effective technique that uses electrostatic forces to produce fibers with diameters ranging from just a few nanometers to several micrometers. Those fibers usually have good features like high surface to volume ratio, flexibility and tunable porosity [31]. A typical electrospinning configuration is composed of three main parts: A high voltage power supply, a syringe and a metallic collector. The power supply electrodes connect to the needle (usually positive) and collector (usually negative). The process is based on the principle that strong electric repulsive forces outweigh the surface tension forces of the polymeric solution [31]. This way, when a sufficiently high electric field is applied to the liquid droplet, this droplet gets charged, and the resulting electrostatic repulsion counteracts the surface tension getting the droplet to stretch and form fibers that are attracted to the collector.

To produce “smart membranes”, one strategy could be the confinement of thermoresponsive microgels in electrospun fibers that could behave as active sites, thus allowing the fabrication of polymeric networks with added functionalities with potential biomedical applications[7]. To do so, a modification of the electrospinning technique is used: Colloidal electrospinning (Figure 1.5). Similar to traditional electrospinning, it uses a colloidal system instead of a homogeneous polymer solution allowing the production of multicomponent fibers with just a single nozzle, being a very good alternative to co-axial electrospinning [32, 33].

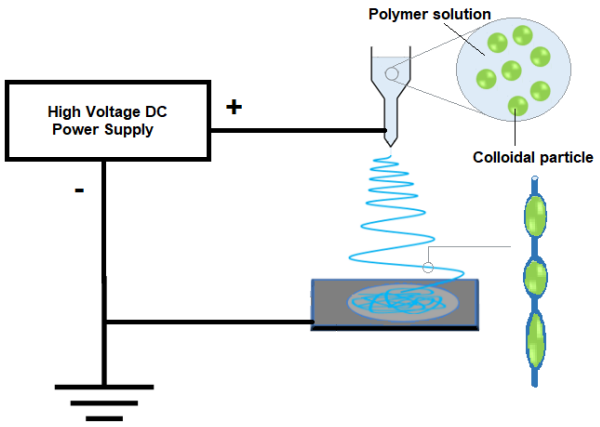

Figure 1.5-Schematic illustration of a colloidal electrospinning setup. The green circles represent the colloid phase.

One of the advantages of using colloidal electrospinning is the different fiber morphologies that can be obtained. There are two main types of morphologies of resulting fibers from this process: '*bead-on-string*' [34] and '*core-shell*' [35]. For the '*bead-on-string*' structures, the dispersed phase has tendency to accumulate in the center of the liquid during its flight in the air [34]. If the electric field is too high, these beads are stretched and displaced from the center resulting in '*spindle-like*' structures [34]. For the '*core-shell*' fibers, the viscosity difference between the particles and the polymeric matrix has a crucial role. During the process, the particles are stretched into elliptical shapes in the fiber's axial direction. If the viscosity difference is not enough, particles do not fully elongate and break up, forming beads instead of a continuous core. There are only a few studies that report the confinement of microgels inside polymeric fibers, but most of them about the incorporation of PNIPAAM microgels [7, 36].

The option to incorporate thermosensitive microgels within the electrospun fibers results in multifunctional fibers with high aspect ratio and porosity and give rise to tunable and functional surfaces. The use of the microgels can also contribute to control the topography of the composite membranes since it has been shown to significantly increase the hydrophobia of an already hydrophobic material. For thermoresponsive hydrophobic material, Wang *et al.* has reported that Poly(N-isopropylacrylamide)/Polystyrene composite nanofiber membranes change their hydrophobicity with the temperature, changing from hydrophilic to super-hydrophobic [36].

This dissertation reports on the development of composite membranes using colloidal electrospinning. The aim target was to develop multifunctional membranes by the confinement of active sites within polymeric fibers. For that, poly(acrylamide -acrylic acid) microgels were synthesized to be used as active sites. The influence of microgel composition, polymeric solution (fiber template/microgel/solvent) as well as electrospinning parameters were studied. Furthermore, the effect of incorporation microgels into the membranes was also studied through the analysis of the mechanical properties of the electrospun membranes.

2 Materials and methods

2.1 Materials

Acrylamide (AAm, Fluka analytical, ≥98%) was used as monomer, *N,N*-methylene bis-acrylamide (MBA, Sigma-Aldrich, 99%) was used as a cross-linker. As initiator, we have chosen 2,2'-Azobis(2-methylpropionamidine) dihydrochloride (AMPA-d, Aldrich, 97%). Acrylic Acid (AAc, Alfa Aesar, tech90% stab.) was purified using vacuum distillation and used as comonomer. Dodecane (Alfa Aesar, 99+%) and Span 80 (Sorbitan Monooleate, Sigma-Aldrich) were employed as organic solvent and surfactant respectively. Ethanol (Scharlau, absolute). The water used in the preparation and characterization of the microgels was Millipore Milli-Q grade.

2.2 Synthesis of Poly(acrylamide) microgels

Microgels were synthesized by means of inverse emulsion polymerization method (water in oil emulsion, w/o) as described in previous studies. ([22] and [23]) For the oil phase, the organic phase and emulsifier were mixed (Dodecane and Span80). In the aqueous phase, the Acrylamide monomer (AA), Acrylic Acid comonomer (AAc) and the cross-linker *N,N*-methylene bis-acrylamide (MBA) were dissolved. Different amounts of AAc were tested (0 wt%, 5wt%, 10wt%, 15 wt%); Table 2.1-Compositions of the synthesized PAA-AAc copolymer microgel describes the different compositions used in this work. Both phases were purged with nitrogen for 10 minutes to remove residual oxygen before starting the reaction. The organic phase was charged into a three-neck round-bottom flask (forming the continuous phase) and the aqueous phase was then added in a controlled manner at 1,5 $ml.h^{-1}$ using a syringe pump (kdScientific) to get droplets with equivalent size. The polymerization was thermally initiated using 2,2'-azobis(2-methylpropionamidine dihydrochloride) (AMPA-d) as initiator. This emulsion was then heated at 50ºC (starting the polymerization reaction) and stirred at 475rpm, under nitrogen atmosphere. After 3 hours of reaction, the flask content was washed and precipitated in ethanol. Finally, the microgels were isolated by centrifugation (Thermo Scientific Multifuge X1R, 10.000 rpm), vacuum dried and stored.
The set-up for the microgel synthesis can be seen in Figure 6.2-Microgel synthesis set-up. (supporting information).

Table 2.1-Compositions of the synthesized PAA-AAc copolymer microgels

Sample PAA-AAc	**Aqueous phase**				**Oil phase**	
	AA (g)	**AAc (g)**	**MBA**	**AMPA-d (g)**	**Dodecane (ml)**	**SPAN 80 (g)**
0%AAc	4	0	0.2	0.04	30	0.5056
5% AAc	4	0.2	0.2	0.04	30	0.5056
10% AAc	4	0.4	0.2	0.04	30	0.5056
15% AAc	4	0.6	0.2	0.04	30	0.5056

2.3 Colloidal-Electrospinning

The electrospinning experiments were carried out using a high voltage supply (Glassman High Voltage, EL, USA), a syringe pump (kdScientific) and a thin foil that was used as collector.
The polymeric solutions used were Polyvinylpyrrolidone (PVP, Sigma-Aldrich, $\bar{M}_w = 1.300.000$) with concentrations of 10 wt% and 14 wt% dissolved in ethanol (Scharlau, absolute). Microgels were also

added to those polymeric solutions (10 wt% and 20 wt% of the PVP mass). In some of the solutions, water was added into the polymeric solutions in order to try to enhance microgel stability.

A 3ml syringe was used for all experiments fitted with a 23-gauge needle. The syringe pump was programmed to deliver the solutions at a flow rate of 0,3 $ml.h^{-1}$ and 1 $ml.h^{-1}$. Two different voltages were applied, 10kV and 15kV, and the distances between the tip of the syringe and collector (TCD) of 12 cm and 20 cm were also used as a variable parameter for this experiment. The environmental conditions were controlled with a relative humidity (RH) kept between 30% to 45% and temperatures of 20°C to 25°C.

2.4 UV cross-linking method

There are several options to crosslink PVP, from high-energy irradiation to temperature treatments. Photocrosslinking of PVP by UV radiation is an inexpensive alternative for crosslinking PVP membranes. This can be achieved by direct irradiation using a low-pressure Hg lamp eliciting 254 nm light.

The achieved crosslinking degree will depend in the irradiation dose and hence in the time that the fiber membranes are irradiated.[8] In this work, all electrospun PVP membranes and composite PVP membranes were crosslinked by UV radiation for 10 minutes at 0.120 joules in a BIO-LINK irradiation system.

2.5 Characterization techniques

For the determination of swelling ability and thermo-responsiveness two techniques were used: (i) dynamic light scattering (DLS) (Horiba Nanopartica Analizer SZ-100 equipped with a 594nm He-Ne laser and a Peltier element to control the temperature) and (ii) optical microscope coupled with a Peltier device. To study the size distribution as a function of the temperature, the dried microgels were dispersed in distilled water and observed in the microscope at different temperatures.

Scanning electron microscopy (SEM) technique was used to visualize the morphology and size of the dried microgel particles. For this technique, the microgel samples were dispersed in deionized water (0.01g/ml), and a drop of this dispersion was deposited in a silicon wafer. After it dried, the samples were sputter-coated with a thin layer of gold and analyzed with a SEM apparatus fitted with Carl Zeiss Auriga CrossBeam system (SEM-FIB).

Fourier transform infrared (FTIR) transmission spectra was used to identify the groups that are involved in the swelling of these poly(acrylamide-acrylic acid) microgels. These analyses were recorded using a FTIR Thermo nicolet 6700 spectrophotometer.

The thermal properties of the synthesized microgel samples were analyzed using the Thermogravimetric analysis technique (TGA), in a Thermogravimetric Analyzer NETZSCH STA 449F3.

Tensile tests were performed to study the mechanical properties of the fiber membranes produced. These fiber membranes were cut into 20x10 mm rectangles and mounted onto a pair of clamps to be stretched at a speed of 1 $mm.min^{-1}$. The tensile testing hardware used was a Rheometric Scientific, Minimat model-Firmware 3.1.

3 Results and Discussion

3.1 PAAm-AAc microgels as active sites

Poly(acrylamide-acrylic acid) polymeric microgels were synthesized by the inverse emulsion polymerization method in the presence of MBA as cross-linking agent, under controlled feeding rate, as it was described in sub-section 2.2 (Synthesis of Poly(acrylamide) Microgels).

As explained before, the mechanism responsible for the swelling and deswelling of the microgels is the hydrogen bonds formed between the acrylic acid and amide functional groups.

Having this in mind, the properties of these thermoresponsive microgels, like VPTT, size and morphology can be controlled by changing their composition. In this work, microgels with different content of AAc (0, 5, 10 and 15 wt.%) were studied with the aim of fine tuning the volume phase transition temperature toward temperatures close to physiological conditions.

3.1.1 Morphology

In the study of the microgels morphology, SEM images give the necessary visual information regarding the homogeneity, microgel particles size and particle size distribution. Figure 3.1 shows representative SEM images corresponding to microgels dispersions containing different acrylic acid content.

As observed from the Figure 3.1, the obtained microgels present a spherical shape as it was previously reported in the literature [22, 27]. However, contrary to what it was expected, SEM images shows a wide dispersity of microgel particle sizes, resulting in a highly polydisperse system.

There are several possible reasons for this to happen, for instance the interaction with impurities or inhibitors. Oxygen is the most common inhibitor, so radical polymerization needs to be done in its total absence, in order to avoid side reactions and to obtain a better Polydispersity Index (PDI). The growing chain will react with molecular oxygen and produce an oxygen radical, which is less reactive, slowing down the propagation rate. Although we purged the solutions with nitrogen before, and the reaction flask was under nitrogen flow during the reaction, as it can be seen in Figure 6.2 (in Supporting Information) oxygen could have entered in the system because we could not seal the flask because of the mechanical stirrer. Another parameter that can also be key factor on the microgel size is the type of initiator, its efficiency and concentration. Different initiators have different rates of decomposition, which can vary depending on the solvent system, as well as its initiator efficiency. The initiator efficiency at initiating polymerization also depends on the monomer [37-39].

In order to better analyze the microgel particle diameter and size distribution SEM images were analyzed using Image J® to determine microgels particle diameters (See Figure 3.2). The obtained size was over an order of magnitude larger than expected. In the literature the sizes reported are little different from each other but always smaller [22, 23, 27]. Poly(acrylamide) microgels present an average particle diameter of 30.48 µm, while for poly (acrylamide-acrylic acid) microgels the average particle diameters were of 42.49 µm, 16.12 µm and 14.53 µm for microgels containing 5, 10 and 15 wt.% of acrylic acid, respectively.

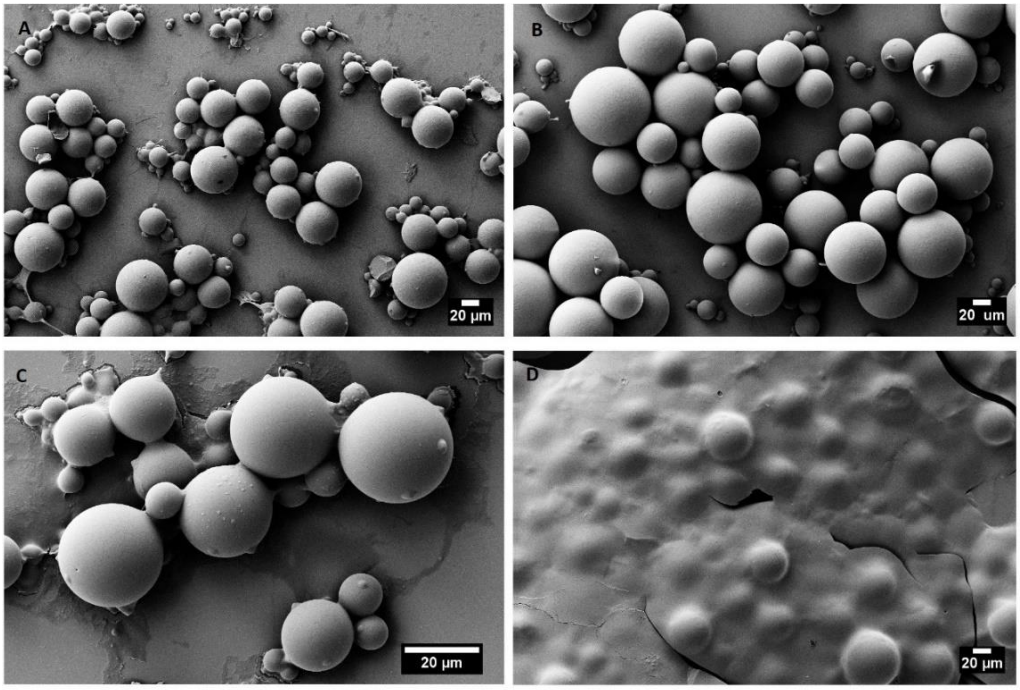

Figure 3.1-SEM micrographs of PAA microgels with 0 wt.% AAc (A), PAA-AAc with 5 wt.% AAc (B), PAA-AAc with 10 wt.% AAc (C) and PAA-AAc with 15 wt.% AAc (D).

In Figure 3.1 are representative SEM images of dried microgels from a diluted microgel dispersions (0.01 $g.ml^{-1}$). The sample of PAA-AAc with 15 wt.% AAc (Figure 3.1, D) was not fully dried, or maybe the organic phase was not completely removed, resulting in the film covering the sample.

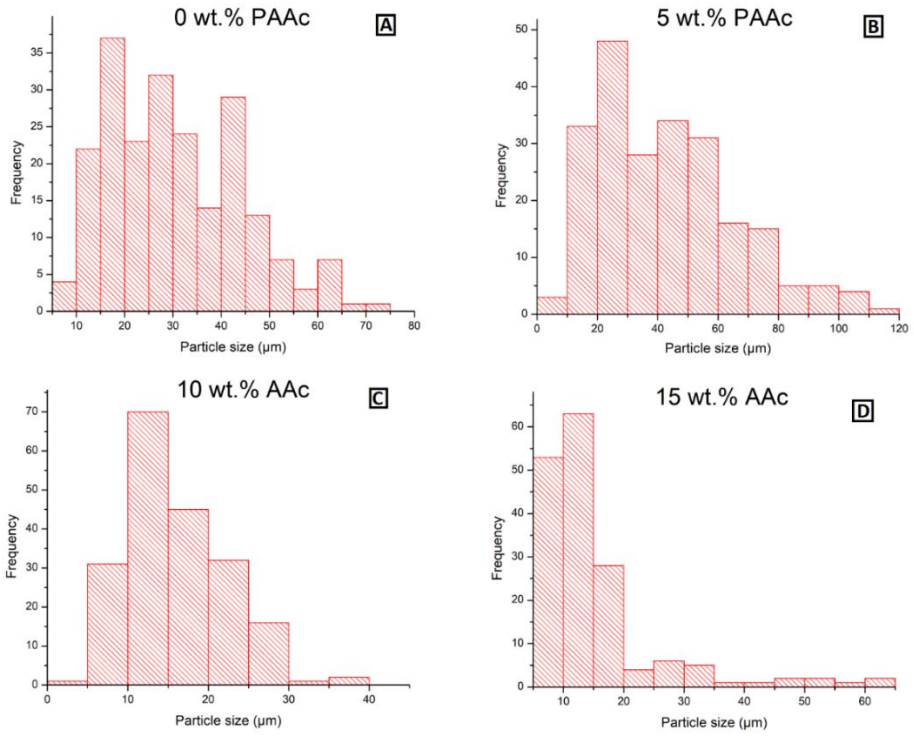

Figure 3.2-Size distribution of the poly(acrylamide-acrylic acid) microgels

For the sake of comparison, Figure 3.3 describes the evolution of the microgel particle size as a function of acrylic acid content. From these graphs, it can be observed that the reference sample, poly(acrylamide) microgel particles, already shows a wide particle size distribution. The incorporation of 5 wt.% of acrylic acid give rise to a microgel dispersion with even higher polydispersity. However, the incorporation of 10 and 15 wt.% of acrylic acid derived in a decrease of the microgel particles size and microgel particles with narrower size distribution. This decrease of particle size with the increase of acrylic acid content is due to the increase of hydrogen bonds between poly(acrylamide) and poly(acrylic acid) and it has already been reported in the literature [22].

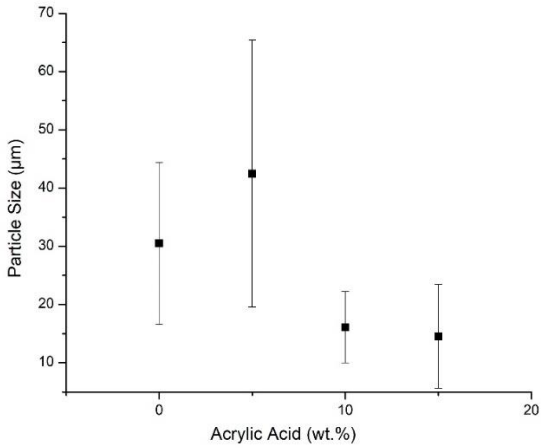

Figure 3.3-Influence of the AAc concentration on the size of the poly(Acrylamide-Acrylic acid) microgels.

3.1.2 Structural characterization

Fourier-transform infrared spectroscopy (ATR-FTIR) technique was used to verify the chemical structure in order to confirm if the synthesis of poly(acrylamide-acrylic acid) microgels was successful. It was also used to identify the groups that might be involved in the swelling of the microgel particles. All microgels with different compositions (0 wt.%, 5 wt.%, 10 wt.%, 15 wt.% AAc) were analysed using ATR-FTIR.

It's well known that PAAc has carboxylic groups which can develop many different intermolecular interactions (hydrogen bonds, electrostatic interaction, dipole-ion…) with other polymers. Many researches have shown that there are strong interactions between PAAc and ionic polymers in aqueous solutions. Intermolecular interactions affect the vibration of groups on polymer segments which can be detected using ATR-FTIR.

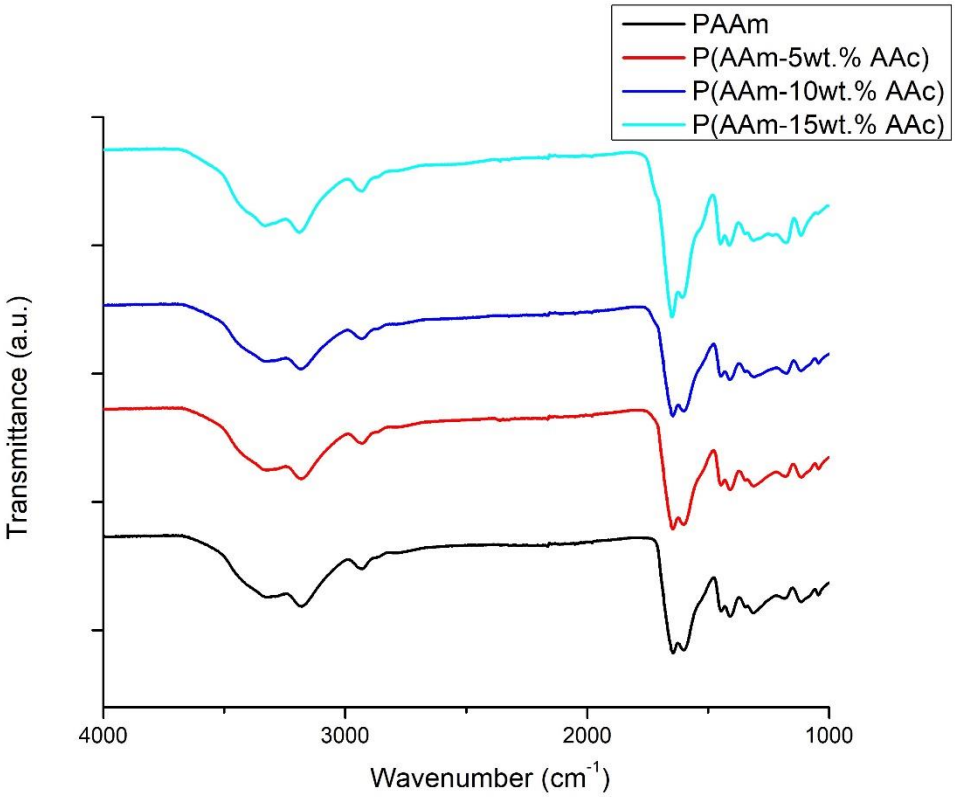

Figure 3.4- (A) *FT-IR spectra of the poly(AAm) and poly(AAm-AAc) microgel samples with 5wt.% AAc, 10wt.% AAc and 15wt.% AAc; (B) Zoom-in for the weak peak due to the cross-linking agent (MBA).*

In Figure 3.4, IR spectra corresponding to Poly(Acrylamide) and Poly(acrylamide-acrylic acid) microgels, containing 5. 10 and 15 wt.% of Acrylic acid are represented.

For microgels of neat poly(acrylamide) the IR spectra shows the stretching of C-H bonds at about 2930 cm^{-1}. According to literature, it is expected a weak peak at 2186 cm^{-1} that is due to the presence of -CN group of the cross-linking agent (MBA). For carbonyl stretching vibration of C=O group connected to the amide group of the acrylamide gives absorption peak at 1645 cm^{-1} and the peak value of about 1600 cm^{-1} is for flexural stretching of -NH amide. The bands at 1441 cm^{-1}, 1351 cm^{-1} and 1300 cm^{-1} are ascribed to the C-N groups of amides [40].

For the poly(acrylamide-acrylic acid) microgels, with the acrylic acid in their composition, in the FTIR spectra the Carbonyl stretching vibration of C=O group of the acrylate unit of the acrylic acid gives an absorption band (shoulder) at 1742 cm^{-1}, and we can see that such shoulder is starting to appear in the spectra for the microgels with 5 wt.% AAc, and it gets clearer as the acrylic acid concentration increases. The band at 1175 cm^{-1} corresponds to the COO^- stretching of acrylate unit. The asymmetric and symmetric stretching of COO^- for the poly(AAm-AAc) samples spectra give absorption peaks at 1580 cm^{-1} and 1448 cm^{-1}, respectively. These results show that the carboxylic groups of PAAc are dissociated into COO^-, which complexes with cationic groups of PAAm through electrostatic interaction to form the co-polymer complexes during the polymerization procedure (Solpan *et al*., 2003) [41].

The band that appears in the range of 3100-3500 cm^{-1} is attributed to O-H groups from hydrogen bonds and is usually associated with water, although we can see a clear increase in intensity of that band for the spectra of the microgel sample containing 15 wt.% AAc. This suggests that the band could also be

related to the hydrogen bonds formed between acrylamide and acrylic acid (responsible for their thermosensitivity) and the tensional stretching of N-H amide, that would confirm the formation of the co-polymer [11].

3.1.3 Thermogravimetric Analysis

Thermogravimetric analysis was carried out to study the thermal stability of the PAAm and P(AAm-AAc) microgels. The weight loss from the thermal decomposition of microgels was analyzed by TGA thermograms (Figure 3.5). The thermogravimetric curves of the copolymers showed three steps for the weight loss, the same as the polyacrylamide homopolymer [42]. The first step occurred in the range of 30–200°C (weight loss was about 6% of the total weight), that corresponds to the evaporation of intra and intermolecular water. The second one occurred in the range of 200–300°C (weight loss was about 16% of the total weight), corresponding to the imine reaction of a small number of the amide groups and the thermal decomposition of hydrophobic side chains. The third one occurred in the range of 300–450 °C (weight loss was about 56% of the total weight) corresponding to the decomposition of amide groups and the degradation of the polymer chains. Beyond 450°C, the copolymer decomposed completely [43].

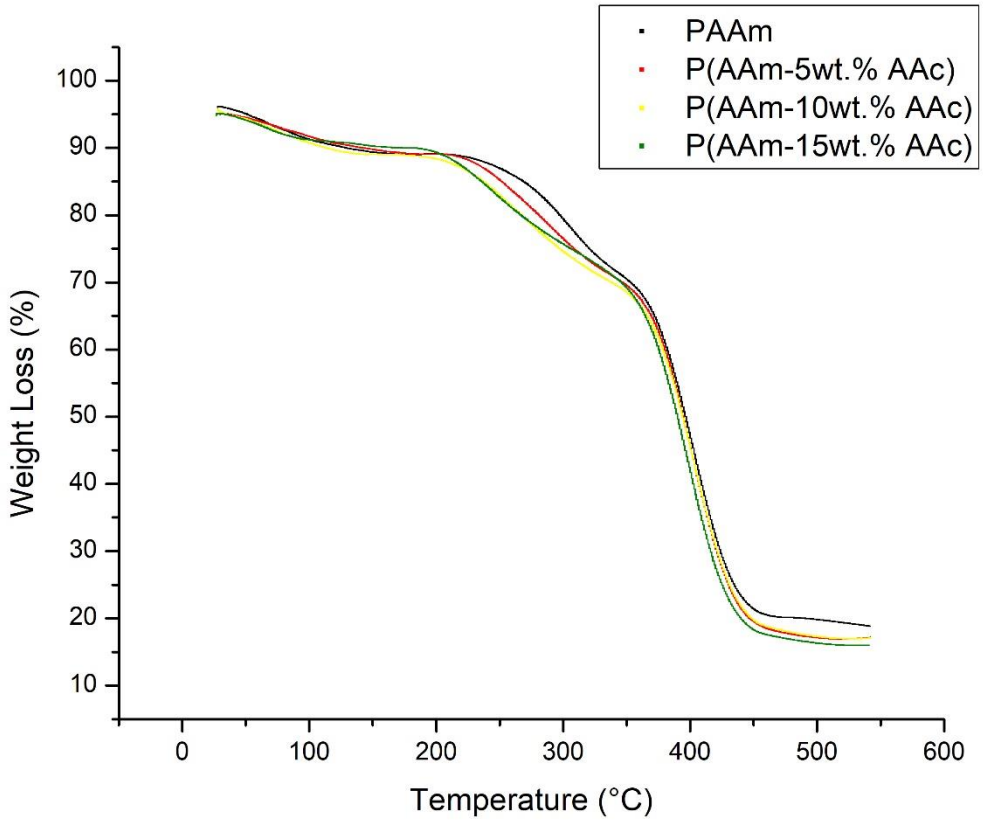

Figure 3.5-Thermal degradation for the microgel samples of PAAm (black) and co-polymer P(AAm-AAc)-5 wt.% (red), P(AAm-AAc)-10 wt.% (yellow), P(AAm-AAc)-15 wt.% (green).

3.1.4 Swelling properties and thermoresponsiveness

As it was previously described in the introduction (1.2.2), positive thermosensitive microgels change their volume with the increase of temperature [22, 23, 27]. The poly(acrylamide-acrylic acid) microgel system swelling is driven by the breaking of the inter-chain interactions. As the temperature increases, the break of the hydrogen bonds creates a hydrophilic front, this is known as zipper effect. This effect is associated with the swelling of these microgels.

The goal of incorporating different quantities of Acrylic acid (AAc) in the system was to fine-tune the transition temperature (VPTT) towards the physiological conditions (~37ºC) so this microgels could be appropriate for potential future biomedical applications.

As stated in the literature, depending on their composition, PAA-AAc microgels should present a VPTT of about 30ºC-45ºC [17, 22, 23, 27].

At room temperature, these microgels are in their collapsed state and their diameters remain constant, but when the temperature increases above the critical temperature (VPTT), the microgels swell and their diameter quickly increases. At higher temperature, the microgels are already at their swollen state and their diameters will attain an equilibrium.

In order to study the microgel swelling properties and confirm the thermosensitivity of the synthesized microgel system we followed two different approaches:

a) Determination of swelling properties using Dynamic Light Scattering

To study the hydrodynamic diameter and swelling behaviour of this synthesized microgels with the temperature, a temperature-programmed dynamic light scattering (DLS) method was used.

This method measures the hydrodynamic diameter (Dh) of sub-micron particles but, as it can be seen in the SEM micrographs, the obtained microgel dispersions present a higher diameter size. To overcome this problem diluted dispersion of microgels (0.01 $g.ml^{-1}$) were filtered using a syringe filter (<400nm) and further measured, in order to ensure that all particles were sub-micron and a narrow particle size distribution.

The information obtained in DLS found at Figure 6.6 (in Supporting information) was not conclusive because the standard deviation values for the measured hydrodynamic diameters were too high. As it is already described in the literature, polyacrylamide microgel sample (0 wt.% acrylic acid) are not thermo-responsive, the hydrodynamic diameter keeps constant with the temperature. As for the poly(acrylamide-acrylic acid) (5 wt.% and 10 wt.% acrylic acid), it should be notice a critical temperature (VPTT) at which the particle starts to swell, but this was not the case of the synthesised microgels. This could be related to the filtering of the samples. Filtering the microgels dispersions (< 400nm) resulted in the elimination of most of the microgels particles, thus making these DLS results very unreliable. Therefore, in order to overcome this problem a second approach using optical microscope was followed.

b) Determination of swelling properties using Optical microscope

As it is described by Serrano *et al.* [23], for the measurement of the swelling of poly(acrylamide-acrylic acid) with sizes of about 5 µm (over a micron), so unable to be measured in DLS, an optical microscope coupled with a Peltier device to control the temperature was used. A drop of the microgel dispersion (0.01 $g.ml^{-1}$) was observed through the microscope while it was heated from 24ºC to 45ºC.

The microscope images obtained were then analysed and the diameters of the microgels were measured using ImageJ. The plot of microgel size with the increase of temperature can be seen in Figure 6.8 (results in supporting information).

The results obtained using this approach were not consistent. As already observed by SEM, the microgel particle size distribution is too wide, making very hard to have results that could be reliable through the entire process. Even worst, with the temperature rise, since the Peltier plate is not completely sealed and water started to evaporate during the temperature ramp experiment. In addition, as observed in Figure 6.7 on the supporting information, at higher temperatures microgels started to aggregate.

The obtained results regarding the analysis of swelling capacity and thermosensitivity were not successful, thus, we could not confirm the thermosensitivity of the synthesised microgels. Although we are not able to measure it, we assume that this UCST-like response still exists in our system, as it has been confirmed in the literature. We believed that the main problem is related to the synthesis and the difficulties found regarding the control of an inert atmosphere, the controlled feeding and the stirring velocities. Several trials were made to solve the problem but no better result was obtained. Further work will be focused in optimizing the synthesis toward lower sizes and monodisperse particle size distributions. The control over the system thermosensitivity can be very important, since there are several potential applications for these systems. In a polymeric membrane, this system can potentially modify the roughness of the fibers, hydrophobicity and wettability, which is also the idea pursued here.

3.2 Production of composite membranes

In the production of fiber membranes by electrospinning method, the morphology and the mean diameter of the fibers (MFD) can be influenced by several parameters that can be gathered in three groups: i) solution parameters; ii) process parameters; iii) environmental conditions.

(i) Polymeric solution concentration influences both viscosity and surface tension. If the solution is too dilute will present low viscosity but the surface tension will difficult the formation of a continuous fiber and it probably will result in many droplets of solution reaching the collector. If on the other hand we have a very viscous solution, the electric field may not be enough to disrupt the viscoelastic forces, which can lead to the formation of fibers with a wide dispersion of diameters [44].

(ii) Electrospinning process parameters also have a major impact on the fibers obtained. For the electric field, if high voltages are applied, the polymer jet suffers greater stretching, leading to the formation of thinner fibers. Applying lower voltages results in reduction of the polymer jet acceleration, leading to an increase time of flight and consequently its stretching ability [45].

Flow rate determines how much polymeric solution is available at the tip of the needle for fiber formation. This not only affects the diameter of the fiber, but also its porosity and shape. So, for a given electric field there is a lower limit of flow rate for the Taylor cone to be stabilized [46].

The distance between the needle tip and collector distance influences the electric field strength as the electric field strength is inversely proportional to this distance. Increasing the tip to collector distance (TCD) may reduce the fiber diameter as there is a greater stretching distance [47]. However beyond a certain distance, the fiber diameter will increase due to the weakened electric field [48].

When this distance is too short it is easily understood that fused fibers may be formed due to insufficient solvent vaporization time, but Ghelich *et al.* observed the same fused fibers when the distance is beyond the optimal range [49].

The TCD also has a major influence on the area of the collected fibers mat. The polymer jet that comes from the droplet in the tip of the needle is accelerated in a straight line-like shape but then it progressively begins to bend, to reduce the density of the surface charge, promoting the jet extension and increasing the surface area. This 'instable whipping' creates a cone, that results in the deposited fiber mats to take a circular shape (base of the cone) [46].

(iii) Environmental conditions are very important because the physical characteristics of the fibers are much influenced by the temperature and humidity. Relative humidity affects the solvent's evaporation and thus the morphology and formation of pores on the fiber surface. Temperature is also very important since it directly affects the polymeric solution properties.

The polymeric solution chosen for this work was polyvinylpyrrolidone (PVP) dissolved in ethanol since it is a well-studied system that has already been reported in the confinement of microgels [50].

De Vrieze *et al.* studied the effect of the environmental parameters on PVP fibers and concluded that with higher relative humidity, the absorption surrounding water results in a slower solidification of fibers, longer jet elongation time and therefore lower fiber diameters [51]. With relative humidity over 60%, the fibers start to fuse with each other, resulting in higher diameters.

The mentioned studies served to determine the optimal electrospinning conditions to obtain PVP electrospun fibers [8, 51].

3.2.1 Confinement microgels of microgels (active sites) into PVP fibers

The objective of this dissertation is the development of composite membranes composed of electrospun fibers containing active sites (microgels) inside the fibers. For that, a modification of the electrospinning technique was used: colloidal electrospinning. This is a cost-effective, simple and versatile technique that instead of electrospinning polymer solutions, a polymeric dispersion is used. In this case it allows the encapsulation of the synthesised Poly(acrylamide-acrylic acid) microgels within polymeric fibres. Considering previously mentioned optimization studies for PVP electrospinning, similar parameters were applied for the confinement of active sites (microgel particles) into PVP fibers. Thus, starting from those conditions, different microgel dispersions (Table 3.1) as well as electrospinning parameters (Table 3.2, Table 3.3) were tested in order to favour the encapsulation of the microgels within the fibers.

Eight different PVP/Microgel dispersions were used (Table 3.1). The concentration of PVP (wt.%) is relative to the mass of the whole solution (for example, the first composition is 10wt.% PVP and 90wt.% ethanol). As for the microgel mass dispersed in the solution, its relative to the PVP mass in the solution (for example, for the first solution in Table 3.1 the mass of microgel dispersed in the solution was 10% of the total weight of PVP in that solution). Also, in some of the solutions, microgels particles were directly dispersed in the PVP/EtOH solution, while in the others, microgels were first dispersed in the water and only then added to the PVP/EtOH solution making the solvent volume 20% water and 80% ethanol. The reason of incorporating water to the solution responds to the need of a more stable colloidal dispersion. In fact, the volume of distilled water used to prepare the microgel dispersions needs to be such that the co-non-solvency of the microgels is ensured. "Co-non-solvency" occurs when two

(perfectly) miscible and competing good solvents (pure water and pure alcohol are both good solvents) for a given polymer, are mixed together and as a result, the same polymer collapses into a compact globule within intermediate mixing ratios [52, 53]. In addition to that, for each of these distinct solutions, many process parameters were also tested in order to study their influence in the fibers morphology, diameter and in the encapsulation of the microgels.

All these variables resulted in 8 depositions for each solution, making it a total of 64 different depositions.

Table 3.1-All the different solution parameters. The microgels used in the production of this set of composite membranes were poly(acrylamide) (0% acrylic acid). (See SEM image in Figure 3.1A)*

PVP (wt.%)	*Microgel ratio (% w/w)	Solvent system
10	10	EtOH/H_2O (80:20)
10	20	EtOH/ H_2O (80:20)
14	10	EtOH/ H_2O (80:20)
14	20	EtOH/ H_2O (80:20)
10	10	EtOH
10	20	EtOH
14	10	EtOH
14	20	EtOH

All the obtained membranes were first observed in the optical microscope in order to pre-select just the ones with potential to have the microgels encapsulated. Some of the images obtained in the optical microscope (Figure 6.9 and Figure 6.10) can be seen in the supporting information.

For the sake of comparison, we will divide the analysis by the solvent system used in the polymer dispersion.

(i) Composite membranes obtained from PVP/MG/EtOH dispersion (no water)

In these first samples, the microgels were added directly into the polymeric solutions without adding water in the solvent system. The prepared solutions and electrospinning parameters are described in table 3.2. In order to confirm microgel confinement and study the influence of the different parameters on the fibers a morphological analysis (SEM) of the fiber membrane obtained was carried out.

Table 3.2-Results for the fiber mats of 14 wt.% PVP in ethanol with 20 % (w/w) of microgels and 10 wt.% PVP in ethanol with 10 % (w/w) of microgels (without water).

Polymeric Solution	Voltage (V)	TCD (cm)	Flow Rate (ml.h^{-1})	Encapsulated	Diameter (μm)
14 wt.% PVP 20 % MG	10	12	0.7	No	1.37±0.32
			0.3	No	1.72±0.48
		20	0.7	No	1.90±0.52
			0.3	No	1.79±0.39
	15	12	0.7	No	1.60±0.71
			0.3	No	1.73±0.64
		20	0.7	No	1.90±0.57
			0.3	No	1.64±0.39
10 wt.% PVP 10% MG	10	12	0.7	No	1.76±0.31
			0.3	Yes*	1.39±0.39
		20	0.7	Yes*	0.81±0.25
			0.3	Yes	1.13±0.32
	15	12	0.7	No	0.85±0.28
			0.3	Yes	1.16±0.31
		20	0.7	Yes*	1.33±0.28
			0.3	Yes	1.05±0.31

*Some microgels seem to be confined yet there are only a few microgels on the membrane and most of the microgels are still outside the fiber.

After analyzing the micrographs, it could be concluded that the microgels were not confined within the fibers. As observed in SEM micrographs (Figure 3.6), even if there were some microgels present in the membrane, most of them were not encapsulated inside the fiber. For the samples produced from the polymeric solution of 10 wt.% PVP, few microgel particles seem to be confined but in very low quantities and with most of the microgels still outside the fibers within the membrane (See Figures 3.6 B)

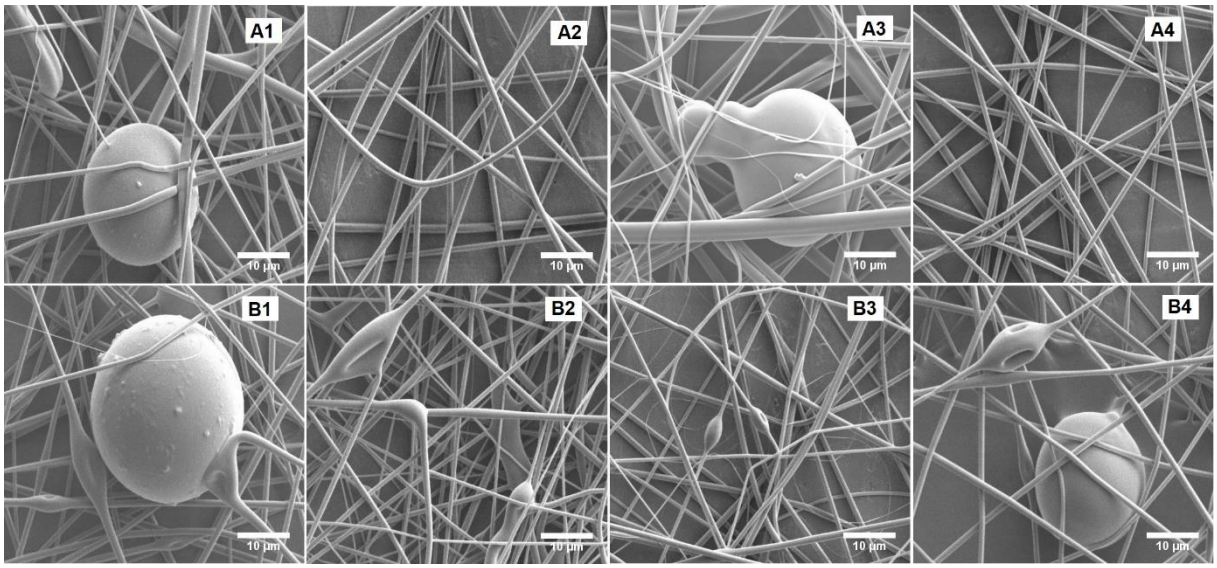

Figure 3.6-Representative SEM micrographs of composite membranes obtained for the polymeric solution of 14 wt.% PVP in ethanol with 20 % (w/w) microgels(A) and 10 wt.% PVP in ethanol with 10% (w/w) microgels (B).

The mean fiber diameter (MFD) were determined from the SEM micrographs using Image J® program and collected in Table 3.2. As expected, it can be seen a decrease in the mean diameter size of the fibers obtained from the solutions with 10 wt.% PVP when compared to the fibers obtained with solutions of 14 wt.%. Thus, confirming that the mean diameter of the fibers decreases with the decrease on polymer concentration.

As mentioned before, 8 different solutions with different compositions were prepared (Table 3.1). From the 4 solutions prepared without water in their solvent system, only 2 were analyzed by SEM (Figure 3.6). The remaining 2 samples without water (10 wt.% PVP with 20% MG and 14 wt.% PVP with 10% MG) were discarded from the previous selection performed through optical microscope already mentioned, which revealed that the resulting fibers presented fiber fusion. Thus, making it impossible to take any reliable data.

(ii) Composite membranes obtained from PVP/MG/EtOH+H_2O dispersion (with water)

In the previous samples, although there was a considerable amount of microgels in the polymeric solution, most of the membranes did not have confined microgels as observed by SEM. This could be due to the fact that microgels were aggregated (and precipitate to the bottom of the syringe) and therefore a phase separation between PVP solution and microgel could occur. In order to make the microgels more stable in the solution, water was added as a dispersant for microgels [53], and the colloidal electrospinning process was repeated for the samples and with the conditions described in Table 3.3.

Table 3.3- Results for the fiber mats of 14 wt.% PVP in ethanol and water with 10% (w/w) of microgels and with 20% (w/w) of microgels.

Polymeric Solution		Voltage (V)	TCD (cm)	Flow Rate (ml.h^{-1})	Encapsulated	Diameter (µm)
14 wt.% PVP	10% MG	10	12	0.7	No	1.61±0.52
				0.3	No	1.48±0.23
			20	0.7	No	1.39±0.54
				0.3	No	1.23±0.27
		15	12	0.7	No	1.40±0.32
				0.3	No	1.04±0.27
			20	0.7	No	1.14±0.63
				0.3	No	1.03±0.28
	20% MG	10	12	0.7	No	1.16±0.30
				0.3	No	1.12±0.19
			20	0.7	No	0.97±0.24
				0.3	No	0.80±0.39
		15	12	0.7	No	0.98±0.27
				0.3	No	0.88±0.23
			20	0.7	No	1.16±0.35
				0.3	No	1.26±0.26
10 wt.% PVP	10% MG	10	12	0.7	Yes	0.87±0.23
				0.3	Yes	0.94±0.20
			20	0.7	Yes	0.79±0.18
				0.3	Yes	0.83±0.28
		15	12	0.7	Yes	0.73±0.16
				0.3	Yes	0.65±0.11
			20	0.7	Yes	0.58±0.08
				0.3	Yes	0.93±0.23
	20% MG	10	12	0.7	Yes	1.02±0.37
				0.3	Yes	0.75±0.14
			20	0.7	Yes	0.74±0.14
				0.3	Yes	0.68±0.17
		15	12	0.7	Yes	0.68±0.14
				0.3	Yes	0.67±0.13
			20	0.7	Yes	0.74±0.15
				0.3	Yes	0.89±0.13

For the solutions with 14 wt.% PVP, even with water in the solvent system, SEM micrographs showed that there were still no microgels confined inside the fibers (Figure 3.7 C, D). However, for the composite membranes produced with the polymeric solutions with 10 wt.% PVP with water in the solvent system, it could be confirmed from SEM micrographs (Figure 3.7 E, F) that the microgels were successfully confined inside the fibers. The MFD of the membranes were also analyzed by means of Image J® and the resulting diameter was collected in Table 3.3.

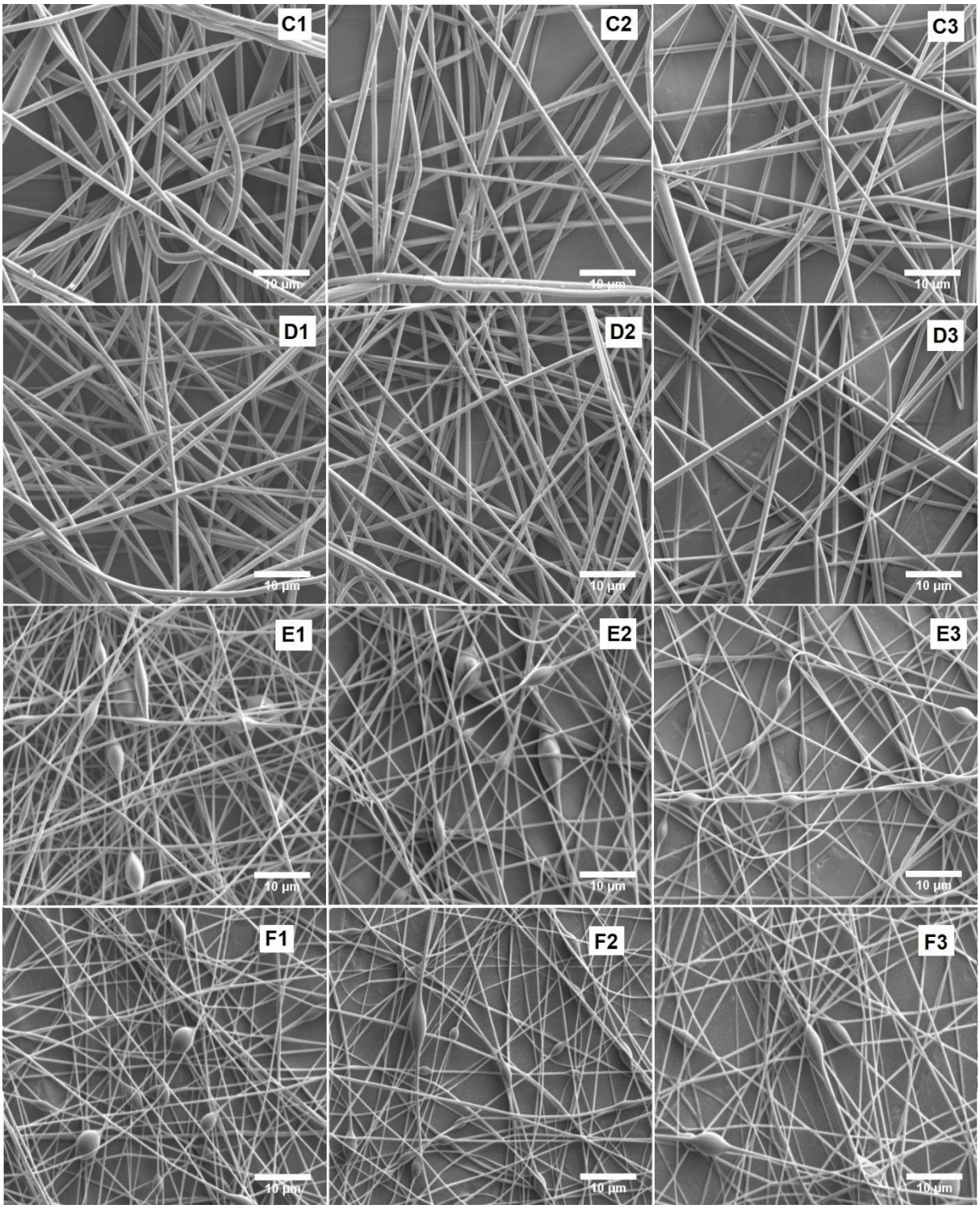

Figure 3.7- Representative SEM micrographs of composite membranes obtained for the polymeric solution of 14 wt.% PVP in ethanol and water with 10 wt.% (C) and 20 wt.% microgels (D) and 10 wt.% PVP with 10 wt.% (E) and 20 wt.% microgels (F)

The obtained results showed that the process parameters do not seem crucial on confining the microgels, since the influence of the process parameters on the diameters are roughly the same with or without water. Also, the solution parameters that did reliably produced composite membranes with confined microgels (Table 3.3), exhibit these confined microgels on every deposition, that is, for all distinct process parameters.

The solution parameters that have shown better results correspond to PVP concentration of 10wt.% with ethanol and water as solvent (Table 3.3). Even for the membranes produced with the solution of 10 wt.% PVP without water in the solvent system (Figure 3.6 B) it was possible to see some microgels confined (although unreliably and not very effective). These results could indicate that the decrease of viscosity of the polymeric solution may result in an easier confinement of the microgels.

The membranes produced by polymeric solutions with water in their composition (Table 3.3) undergo a clear decrease in size of the fibers when compared to the ones with only ethanol as solvent (Table 3.2). In this case the presence of water may decrease the whole polymer chain entanglements for which the viscoelastic force is decreased allowing the production of thinner fibers due to the electrostatic stretching forces of the process.

3.2.2 Analysis of the mechanical properties. Influence of the microgels

To study the microgels influence in the mechanical properties of the PVP membranes, tensile tests of the composite electrospun membranes were performed.

In Figure 3.8 (A) representative strain/stress curves of the performed tensile test corresponding to electrospun membranes prepared from 10% PVP/EtOH solution, and composite membranes of 10% PVP/EtOH with 10 and 20 wt.% of microgel content are shown. As already concluded from morphological studies (See Figure 3.6), these composite membranes contain microgels particles within the membrane but those microgels are not confined within PVP fibers.

The results obtained in these tensile experiments are summarized in Figure 3.8 (B) where average values of the Yield Strength (σ_y), Young's Modulus (E), Ultimate Tensile Strength (UTS) and Elongation at break (ε) are shown (at least 10 measurements for each sample). As observed from Figure 3.8 (both A and B), the incorporation of microgels to the system give rise to stronger membranes, since Young's modulus, as well as elongation at break and UTS increase with the presence of microgels.

A

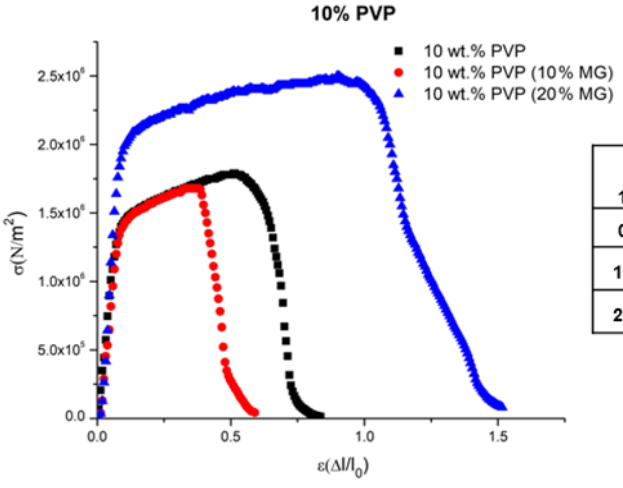

B

PVP 10wt.%	E (MPa)	σ_y (MPa)	UTS (MPa)	ε
0% MG	24.27±3.97	1.52±0.43	1.64±0.23	0.81±0.167
10% MG	25.00±7.94	1.65±0.44	1.62±0.44	0.517±0.105
20% MG	28.38±14.7	1.81±0.49	2.22±0.61	1.735±0.302

Figure 3.8-(A) Representative Stress/strain curves for 10 wt.% PVP composite membranes containing 0, 10 and 20% microgels (MG) without water in their composition. (B) Table with Mechanical properties obtained from the mechanical tests

A similar study was carried out for composite membranes in which microgels are indeed confined within the PVP fibers. In this case, tensile tests were performed to the electrospun membranes prepared from

10% PVP/EtOH/H_2O solution, and 10% PVP/EtOH/H_2O solution containing 10 and 20% of microgels as shown in Figure 3.9. The results obtained from these strain/stress curves are collected in the table shown in Figure 3.9 (B). In this case, the incorporation of 20% of microgel increase the mechanical properties of the membrane. This is not the case of the sample containing 10% of microgels that give rise to values similar or even slightly lower than those obtained for the reference sample (without microgels).

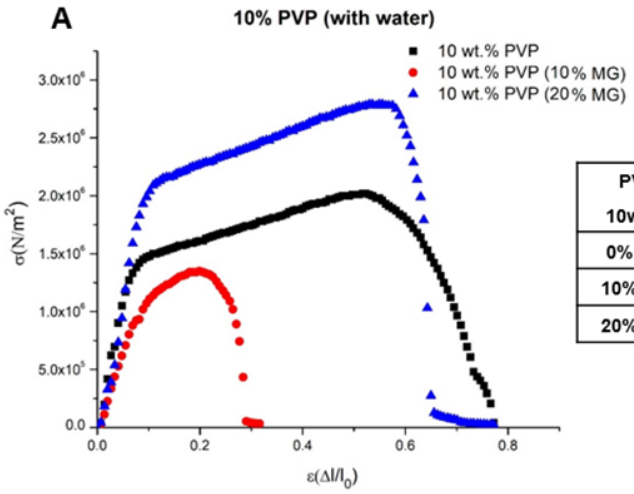

B

PVP 10wt.%	E (MPa)	σ_y (MPa)	UTS (MPa)	ε
0% MG	19.39±4.6	1.15±0.29	1.63±0.44	0.785±0.135
10% MG	15.9±5.8	1.17±0.16	1.34±0.16	0.302±0.062
20% MG	22.63±7.48	1.92±0.45	2.30±0.61	0.690±0.105

Figure 3.9-(A) Representative Stress/strain curves for 10 wt.% PVP composite membranes containing 0, 10 and 20% microgels (MG) with water in their composition. (B) Table with Mechanical properties obtained from the mechanical tests

A general conclusion that can be drawn from this experiment (whether microgels are confined or not within the fibres) is that in both cases the incorporation of microgel particles contribute to improve the mechanical properties of the membrane. This increase in the mechanical properties is probably owing to the interlocking network of the microgels in the composite membranes. A similar effect has already been reported by Le *et al.* with the addiction of hydroxyapatite particles in a polymeric membrane [54]. By comparing the composite membranes without water (Figure 3.8) with the ones with water (Figure 3.9), it can be concluded that on average there is a small decrease on the mechanical properties for the membranes with encapsulated microgels (with water). This decrease of the mechanical properties is probably due to the presence of water in the system. Even when comparing the samples without microgels (10wt% PVP/EtOH 0%MG and 10wt% PVP/EtOH/H_2O 0%MG), there is also a clear decrease of mechanical properties for the membrane produced with water in the solvent system. This infers that during the electrospinning process, the fibers cannot dry completely and consequently resulting in slightly more fragile fibers. Also, the fiber diameters are smaller in the membranes produced from the polymeric solution with water in the solvent system (see Table 3.3). In Figure 3.9 (B) a decrease in the mechanical properties for the membrane prepared from the solution containing 10 wt.% PVP and 10% MG can be observed. However, and before taking any more conclusions, there are some factors that must be taken into account such as relative humidity (HR) and temperature that may also influence the obtained results, not only during the electrospinning process but also while these tensile tests were performed. Also, the electrospinning process is influenced by various inter-related and independent

variables, minute differences in the collection of the membrane may result in changes in the packaging of the fibers in the membrane, influencing its failure mechanism. For thin membranes, it is likely that it will fail through necking and catastrophic failure at a maximum load. However, in thicker membranes, it is more likely that it is made of several thin layers of fibers and its failure will be through delamination of the individual layers [55].

4 Conclusions and Future Perspectives

This work was mainly focused on the production of smart membranes. For this purpose, we proceeded to the confinement of thermosensitive microgels as active sites inside electrospun polymeric fibers produced by colloidal electrospinning.

Poly(acrylamide) and poly(acrylamide-acrylic acid) microgels were prepared through inverse emulsion polymerization. The information found in the literature about this PAAm-PAAc microgel systems reports about their thermosensivity. However, due to the size and wide dispersion of the diameters obtained for these microgels, we could not use DLS technique to confirm their thermosensivity. Another method found in the literature was also tried but the results obtained were not very reliable either. Therefore, it was not possible to confirm the thermosensivity of the microgels. We believe that the main problem is probably related to the synthesis of the microgels that should be optimized as further work.

For the confinement of the microgels, many different solutions parameters and different electrospinning parameters were tested and it was concluded that the solution parameters were very important, and that water was crucial to the confinement of the microgels in the fibers as it lowers the viscosity of the polymeric solution and contributes to the stability of the microgel dispersions.

Tensile tests were performed to study the influence of the solution parameters on the mechanical properties of the composite membranes. The results obtained showed that water decreases the mechanical properties of the membranes, while the addiction of microgels on the polymeric solution clearly enhanced the resulting composite membrane's mechanical properties.

Considering that it was possible to confine the microgels within the fibers, which was the main objective of this dissertation, further work need to be done in optimization of the microgel synthesis in order to obtain lower sizes and monodisperse particle size distributions.

Regarding the composite membrane, it could be interesting to characterize their surface tension since these membranes with confined thermoresponsive microgels can not only modify the topography of the fibers but also its hydrophobicity.

This system is very versatile, allowing the confinement different active sites on the membranes with different functionalities in order to respond in different ways depending on the external-stimuli. For instance, as future work, the syntheses of hybrid microgels with magnetic nanoparticles would be performed to obtain dual-responsive (temperature and magnetic field) composite membranes.

5 References

[1] Ke, C.-J., et al., *Smart Multifunctional Hollow Microspheres for the Quick Release of Drugs in Intracellular Lysosomal Compartments.* Angewandte Chemie International Edition, 2011. 50(35): p. 8086-8089.

[2] Im, J.S., B.C. Bai, and Y.-S. Lee, *The effect of carbon nanotubes on drug delivery in an electro-sensitive transdermal drug delivery system.* Biomaterials, 2010. 31(6): p. 1414-1419.

[3] Wang, T.-M., et al., *An Accurately Controlled Antagonistic Shape Memory Alloy Actuator with Self-Sensing.* Sensors, 2012. 12(6): p. 7682.

[4] Wu, D.Y., S. Meure, and D. Solomon, *Self-healing polymeric materials: A review of recent developments.* Progress in Polymer Science, 2008. 33(5): p. 479-522.

[5] Thakur, V.K. and M.R. Kessler, *Self-healing polymer nanocomposite materials: A review.* Polymer, 2015. 69: p. 369-383.

[6] Hong, C.-Y., et al., *Application of FBG sensors for geotechnical health monitoring, a review of sensor design, implementation methods and packaging techniques.* Sensors and Actuators A: Physical, 2016. 244(Supplement C): p. 184-197.

[7] Marques, S.C.S., et al., *Confinement of thermoresponsive microgels into fibres via colloidal electrospinning: experimental and statistical analysis.* RSC Advances, 2016. 6(80): p. 76370-76380.

[8] Faria, J.M., *Production and optimization of hybrid fibrillary gels by colloidal electrospinning*, in *DCM*2016, FCT-UNL.

[9] Baker, W.O., *Microgel, a New Macromolecule. Relation to Sol and Gel as Structural Elements of Synthetic Rubber.* Rubber Chemistry and Technology, 1949. 22(4): p. 935-955.

[10] Thorne, J.B., G.J. Vine, and M.J. Snowden, *Microgel applications and commercial considerations.* Colloid and Polymer Science, 2011. 289(5): p. 625.

[11] Nesrinne, S. and A. Djamel, *Synthesis, characterization and rheological behavior of pH sensitive poly(acrylamide-co-acrylic acid) hydrogels.* Arabian Journal of Chemistry, 2017. 10(4): p. 539-547.

[12] Qin, Y., et al., *Near-infrared light remote-controlled intracellular anti-cancer drug delivery using thermo/pH sensitive nanovehicle.* Acta Biomaterialia, 2015. 17(Supplement C): p. 201-209.

[13] Wadajkar, A.S., et al., *Prostate cancer-specific thermo-responsive polymer-coated iron oxide nanoparticles.* Biomaterials, 2013. 34(14): p. 3618-3625.

[14] Ahn, S.-k., et al., *Stimuli-responsive polymer gels.* Soft Matter, 2008. 4(6): p. 1151-1157.

[15] Zhai, L., *Stimuli-responsive polymer films.* Chemical Society Reviews, 2013. 42(17): p. 7148-7160.

[16] Stuart, M.A.C., et al., *Emerging applications of stimuli-responsive polymer materials.* Nat Mater, 2010. 9(2): p. 101-113.

[17] Echeverria, C. and C. Mijangos, *Effect of Gold Nanoparticles on the Thermosensitivity, Morphology, and Optical Properties of Poly(acrylamide-acrylic acid) Microgels.* Macromol Rapid Commun, 2010. 31(1): p. 54-8.

[18] Smeets, N.M.B. and T. Hoare, *Designing responsive microgels for drug delivery applications.* Journal of Polymer Science Part A: Polymer Chemistry, 2013. 51(14): p. 3027-3043.

[19] Constantin, M., et al., *Lower critical solution temperature versus volume phase transition temperature in thermoresponsive drug delivery systems.* Express Polymer Letters, 2011. 5(10): p. 839-848.

[20] Saunders, B.R., *On the Structure of Poly(N-isopropylacrylamide) Microgel Particles.* Langmuir, 2004. 20(10): p. 3925-3932.

[21] McPhee, W., K.C. Tam, and R. Pelton, *Poly (N-isopropylacrylamide) latices prepared with sodium dodecyl sulfate.* Journal of colloid and interface science, 1993. 156(1): p. 24-30.

[22] Echeverria, C., D. López, and C. Mijangos, *UCST Responsive Microgels of Poly(acrylamide−acrylic acid) Copolymers: Structure and Viscoelastic Properties.* Macromolecules, 2009. 42(22): p. 9118-9123.

[23] Serrano-Ruiz, D., et al., *Influence of the inter-chain hydrogen bonds on the thermoresponsive swelling behavior of UCST-like microgels.* Polymer, 2013. 54(18): p. 4963-4971.

[24] Owens, D.E., et al., *Thermally Responsive Swelling Properties of Polyacrylamide/Poly(acrylic acid) Interpenetrating Polymer Network Nanoparticles.* Macromolecules, 2007. 40(20): p. 7306-7310.

[25] Bouillot, P. and B. Vincent, *A comparison of the swelling behaviour of copolymer and interpenetrating network microgel particles.* Colloid and Polymer Science, 2000. 278(1): p. 74-79.

[26] Okano, T., *Molecular design of temperature-responsive polymers as intelligent materials*, in *Responsive Gels: Volume Transitions II*, K. Dušek, Editor 1993, Springer Berlin Heidelberg: Berlin, Heidelberg. p. 179-197.

[27] Ruiz, D.S., et al., *Polymer Diffusion in Microgels with Upper Critical Solution Temperature as Studied by Incoherent Neutron Scattering.* Journal of Physics: Conference Series, 2014. 549: p. 012012.

[28] Jo, E., et al., *Core-Sheath Nanofibers Containing Colloidal Arrays in the Core for Programmable Multi-Agent Delivery.* Advanced Materials, 2009. 21(9): p. 968-972.

[29] Kim, Y.-J., M. Ebara, and T. Aoyagi, *A Smart Hyperthermia Nanofiber with Switchable Drug Release for Inducing Cancer Apoptosis.* Advanced Functional Materials, 2013. 23(46): p. 5753-5761.

[30] James, R., et al., *Tendon tissue engineering: Adipose 1 derived stem cell and GDF-5 mediated regeneration using electrospun matrix systems.* Biomedical materials (Bristol, England), 2011. 6(2): p. 025011-025011.

[31] Bhardwaj, N. and S.C. Kundu, *Electrospinning: A fascinating fiber fabrication technique.* Biotechnology Advances, 2010. 28(3): p. 325-347.

[32] Xu, X., et al., *Preparation of Core-Sheath Composite Nanofibers by Emulsion Electrospinning.* Macromolecular Rapid Communications, 2006. 27(19): p. 1637-1642.

[33] Crespy, D., K. Friedemann, and A.-M. Popa, *Colloid-Electrospinning: Fabrication of Multicompartment Nanofibers by the Electrospinning of Organic or/and Inorganic Dispersions and Emulsions.* Macromolecular Rapid Communications, 2012. 33(23): p. 1978-1995.

[34] Qi, et al., *Encapsulation of Drug Reservoirs in Fibers by Emulsion Electrospinning: Morphology Characterization and Preliminary Release Assessment.* Biomacromolecules, 2006. 7(8): p. 2327-2330.

[35] Elahi, M.F. and W. Lu, *Core-shell Fibers for Biomedical Applications-A Review.* Journal of Bioengineering & Biomedical Science, 2013. 03(01).

[36] Wang, N., Y. Zhao, and L. Jiang, *Low-Cost, Thermoresponsive Wettability of Surfaces: Poly(N-isopropylacrylamide)/Polystyrene Composite Films Prepared by Electrospinning.* Macromolecular Rapid Communications, 2008. 29(6): p. 485-489.

[37] Goto, A. and T. Fukuda, *Effects of Radical Initiator on Polymerization Rate and Polydispersity in Nitroxide-Controlled Free Radical Polymerization.* Macromolecules, 1997. 30(15): p. 4272-4277.

[38] Ragimov, A.V., et al., *Effect of initiator type on the composition and molecular mass distribution of p-benzoquinone polymerization products.* Polymer Science U.S.S.R., 1989. 31(1): p. 104-109.

[39] Walling, C., *Initiator efficiency in radical polymerization.* Journal of Polymer Science, 1954. 14(74): p. 214-217.

[40] Ghorbaniazar, P., et al., *Preparation of Poly Acrylic Acid-Poly Acrylamide Composite Nanogels by Radiation Technique.* Adv Pharm Bull, 2015. 5(2): p. 269-75.

[41] Şolpan, D., et al., *Adsorption of methyl violet in aqueous solutions by poly(acrylamide-co-acrylic acid) hydrogels.* Radiation Physics and Chemistry, 2003. 66(2): p. 117-127.

[42] Yang, M.-H., *The Two-Stages Thermal Degradation of Polyacrylamide.* Polymer Testing, 1998. 17(3): p. 191-198.

[43] Al-Sabagh, A.M., et al., *Synthesis and characterization of high molecular weight hydrophobically modified polyacrylamide nanolatexes using novel nonionic polymerizable surfactants.* Egyptian Journal of Petroleum, 2013. 22(4): p. 531-538.

[44] Sill, T.J. and H.A. von Recum, *Electrospinning: Applications in drug delivery and tissue engineering.* Biomaterials, 2008. 29(13): p. 1989-2006.

[45] Chen, M., et al., *Magnetic electrospun fluorescent polyvinylpyrrolidone nanocomposite fibers.* Polymer, 2012. 53(20): p. 4501-4511.

[46] Newsome, T.E. and S.V. Olesik, *Electrospinning silica/polyvinylpyrrolidone composite nanofibers.* Journal of Applied Polymer Science, 2014. 131(21): p. n/a-n/a.

[47] Mazoochi, T., et al., *Investigation on the Morphological Characteristic of Nanofiberous Membrane as Electrospun in the Different Processing Parameters*. Vol. 3. 2012. 2-9.

[48] Ding, W., et al., *Manipulated Electrospun PVA Nanofibers with Inexpensive Salts.* Macromolecular Materials and Engineering, 2010. 295(10): p. 958-965.

[49] Ghelich, R., M. Keyanpour Rad, and A. Youzbashi, *Study on Morphology and Size Distribution of Electrospun NiO-GDC Composite Nanofibers*. Vol. 10. 2015. 12-19.

[50] Díaz, J.E., et al., *Absorption Properties of Microgel-PVP Composite Nanofibers Made by Electrospinning.* Macromolecular Rapid Communications, 2010. 31(2): p. 183-189.

[51] De Vrieze, S., et al., *The effect of temperature and humidity on electrospinning.* Journal of Materials Science, 2008. 44(5): p. 1357.

[52] Mukherji, D., et al., *Co-non-solvency: Mean-field polymer theory does not describe polymer collapse transition in a mixture of two competing good solvents.* The Journal of Chemical Physics, 2015. 142(11): p. 114903.

[53] Crowther, H.M. and B. Vincent, *Swelling behavior of poly- N-isopropylacrylamide microgel particles in alcoholic solutions.* Colloid and Polymer Science, 1998. 276(1): p. 46-51.

[54] Le, H.R., et al., *Fabrication and mechanical properties of chitosan composite membrane containing hydroxyapatite particles.* Journal of Advanced Ceramics, 2012. 1(1): p. 66-71.

[55] ASTM, *Standard Test Method for Tensile Properties of Thin Plastic Sheeting*, 2012, ASTM: West Conshohocken, PA.

[56] Harwood, L.M. and C.J. Moody, *Experimental Organic Chemistry: Principles and Practice*1989: Blackwell Scientific Publications.

6 Supporting Information

6.1 Vacuum distillation

In order to keep liquid monomers (like acrylic acid) stable, small amounts of inhibitors may be used to increase their shelf life. For proper monitoring of the reaction, these inhibitors should be removed. The process chosen to remove the inhibitors was the vacuum distillation. This process is used to lower the boiling temperatures of the compounds and so to avoid decomposition. It works on the principle that boiling occurs when the pressure above the liquid to be distilled is lower than its vapor pressure. [56]

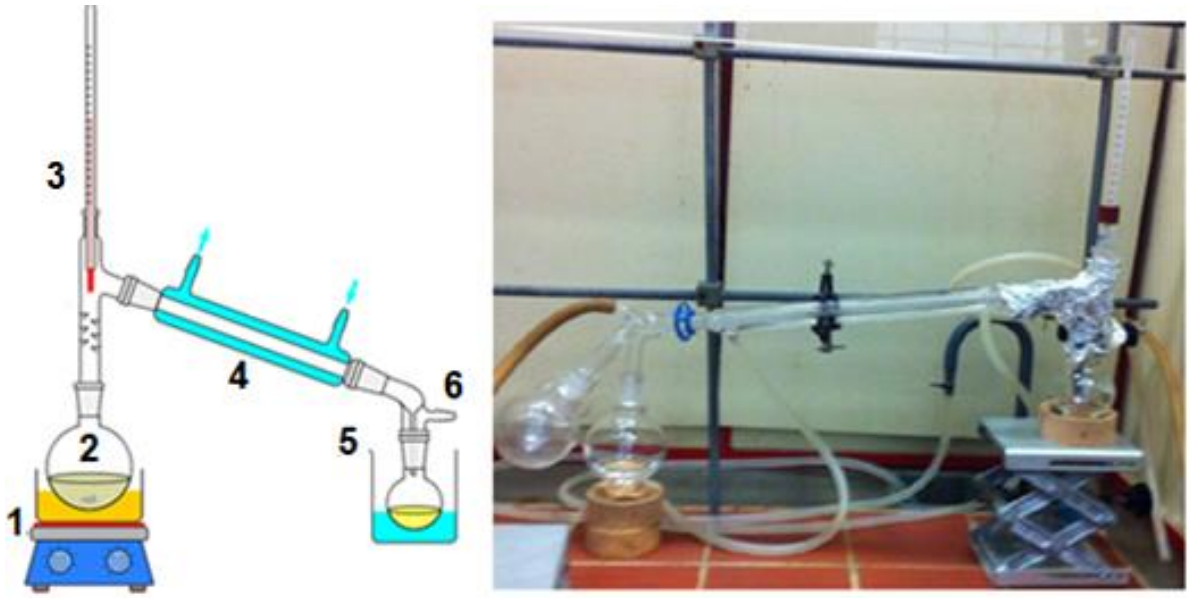

Figure 6.1- Vacuum distillation set-up; 1-heater; 2- round bottom flask; 3- thermometer; 4- condenser; 5-round bottom flask; 6- Vacuum inlet;- adapted from [56]

6.2 Synthesis of Poly(acrylamide) microgels

Figure 6.2-Microgel synthesis set-up.

Microgels were synthesized by means of inverse emulsion polymerization method (water in oil emulsion, w/o), in which the aqueous phase is dispersed into the oil phase, that constitutes the continuous phase, forming droplets.

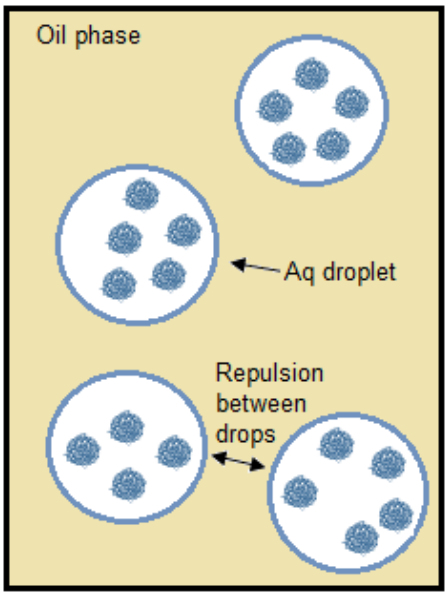

Figure 6.3-Microgels in inverse emulsion (w/o)

6.3 Polymerization reaction

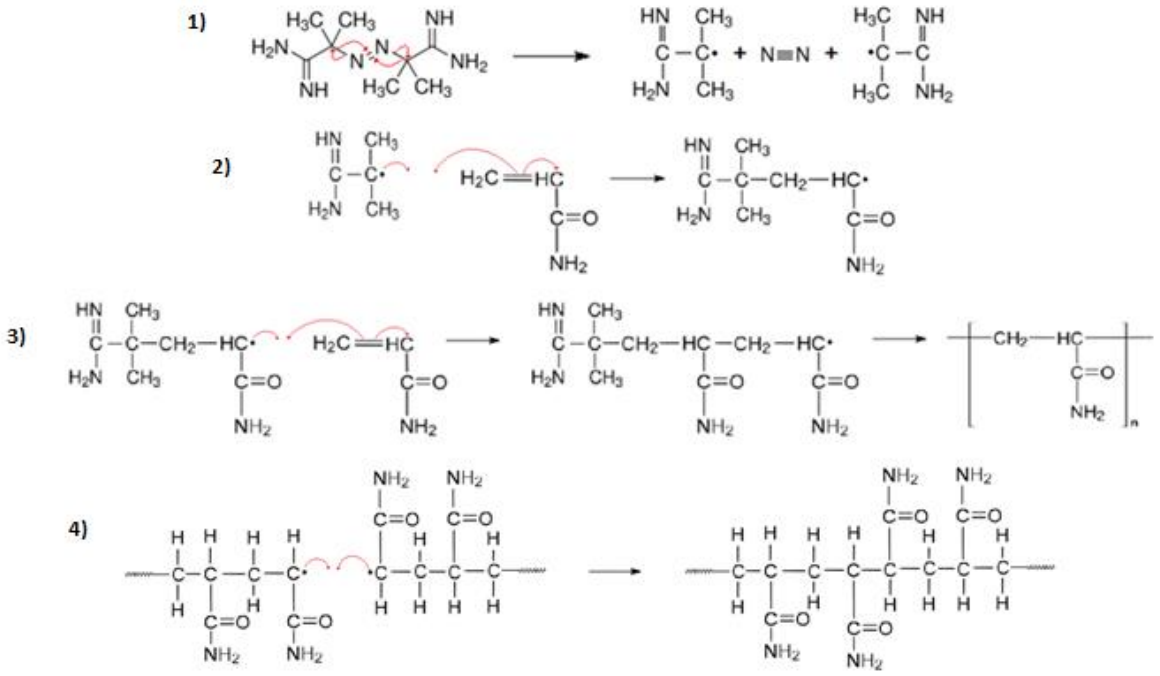

Figure 6.4-Polymerization reaction scheme. 1) and 2) Thermal activation of the initiator/Initiation; 3) Propagation; 4) Termination

The formation of microgels was due to an addition polymerization, more specifically, a free-radical polymerization because the process starts with the activation of molecules called initiators. In this reaction, the first step is the initiation (1) where the thermal activation of an initiator molecule (2,2'-Azobis(2-methylpropionamidine) dihydrochloride) results in the formation of two free radicals and a single nitrogen molecule. The single dot alone represents an unpaired electron. In the second part of the initiation step (2), the free radicals attack the double bond of the monomer (Acrylamide), breaking it. Then the monomer links to the free radical molecule and the unpaired electron goes to the carbon atom in the monomer. Most of the time of the reaction is spent in this next step, propagation (3), the activated molecule attacks the double bond of a new monomer molecule and attaches to it while the unpaired electron moves to the carbon of the newly-attached monomer. This growing chain will continue to attack and attach monomer molecules again and again to form a long polymer chain.

But this chain reaction cannot go on forever, it ends in the last step, termination (4), when a growing chain joins with another free radical (another growing polymer chain or the original free radicals) to form a stable bond.

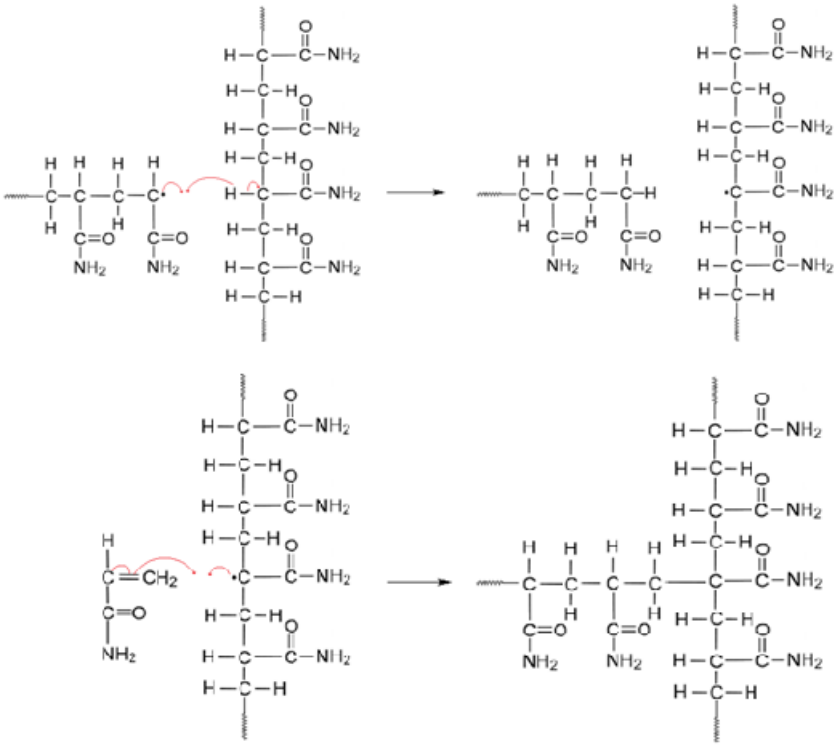

Figure 6.5-Termination that leads to chain branching

There may be also a termination process that causes the chain branching of the growing polymeric chain as shown in Figure 6.5-Termination that leads to chain branching.

6.4 Determination of swelling properties using Dynamic Light Scattering

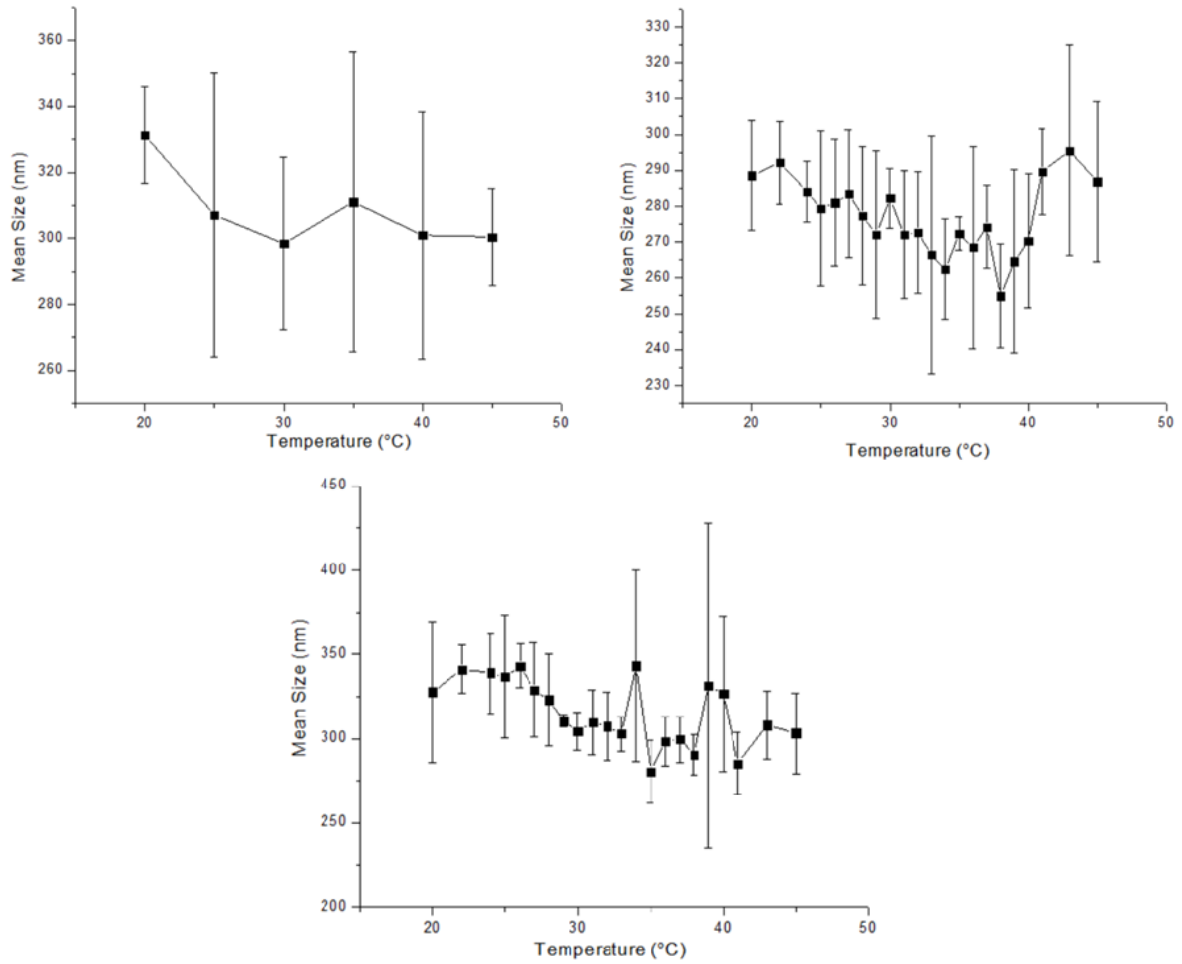

Figure 6.6- Evolution of the hydrodynamic diameter (Dh) with temperature for simple Polyacrylamide microgels (0% AAc) and PAA-AAc 5% AAc, 10% AAc

6.5 Determination of swelling properties using Optical Microscope

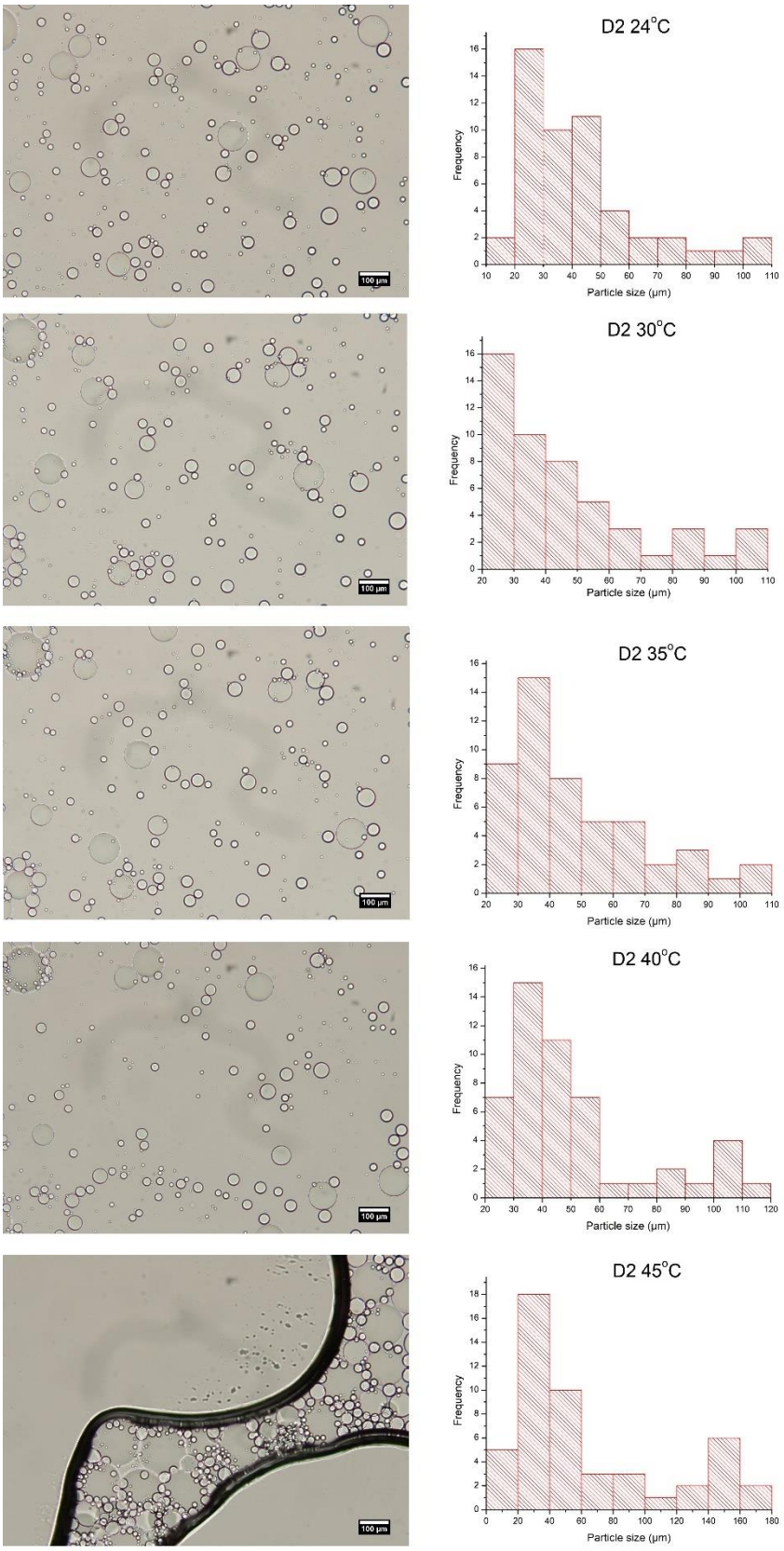

Figure 6.7-Samples seen through the Optic Microscope with increasing temperature.

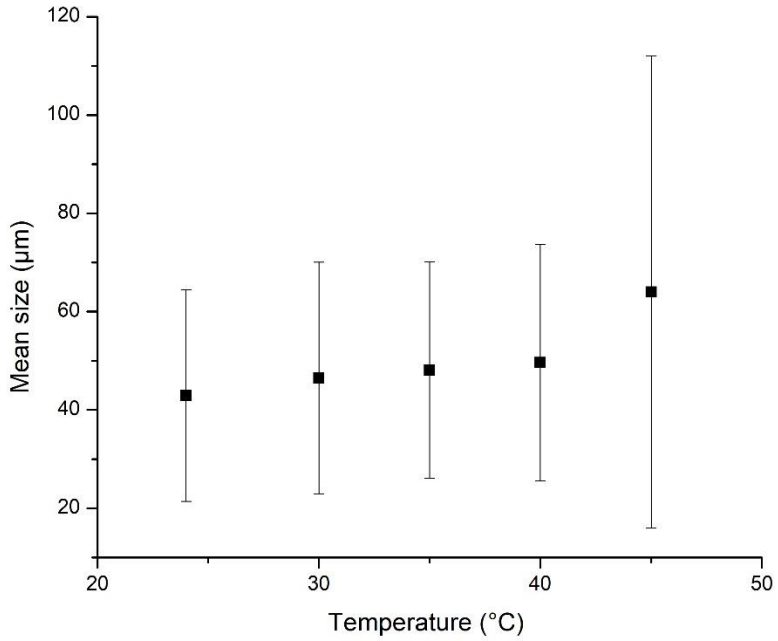

Figure 6.8-Influence of the temperature on the swelling of the microgels with 5 wt.% AAc

6.6 Membrane pre-selection with Optical Microscope

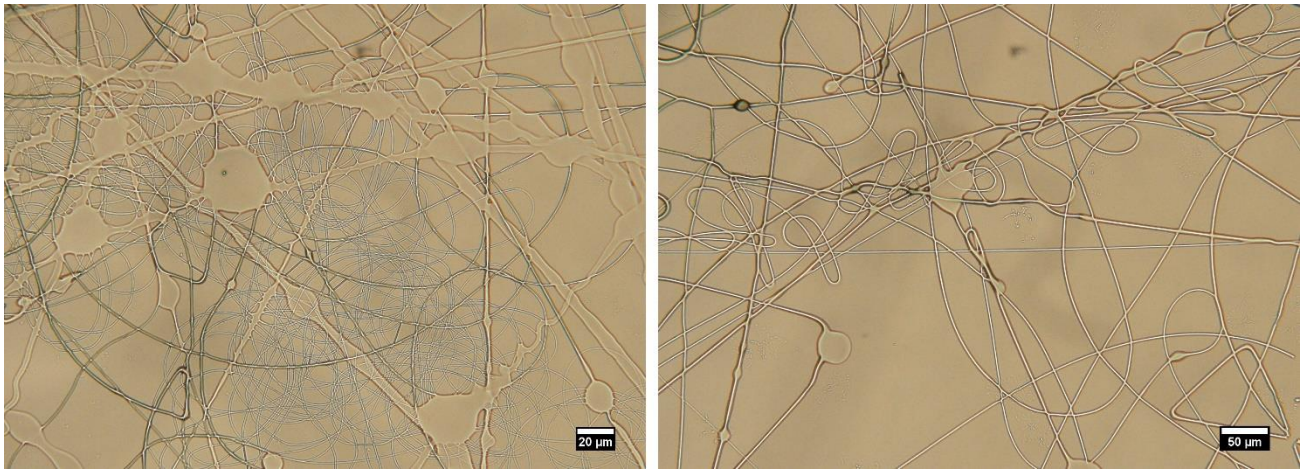

Figure 6.9-Microscopic image of fused fibers for the polymeric solution with 10 wt.% PVP in ethanol with 20 % w/w MG

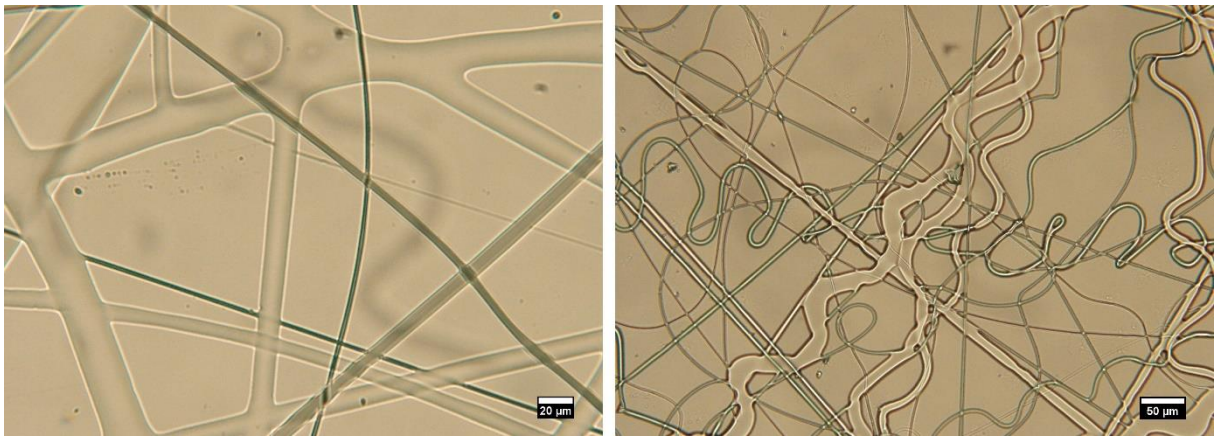

Figure 6.10-Microscopic image of fused fibers for the polymeric solution with 14 wt.% PVP in ethanol with 10 % w/w MG